Taxonomy and phylogeny of *Diaporthales* in Guizhou Province, China

Yong Wang (yongwangbis@aliyun.com)

Research

Keywords: 1 new genus, 8 new species, Chrysofolia, Diaporthe, Foliocryphiaceae

Posted Date: October 24th, 2022

DOI: https://doi.org/10.21203/rs.3.rs-2198153/v1

Abstract

During a study of fungi isolated from plant material in Guizhou Province, China, we identified 26 strains of *Diaporthales*. These were identified from phylogenetic analyses of ITS, LSU, *rpb2*, *tef1* and *tub2* gene sequence data, coupled with morphological studies. The isolated fungi included a new genus in *Foliocryphiaceae* isolated from *Acer palmatum* and *Hypericum patulum*, a new species of *Chrysofolia* isolated from *Coriaria nepalensis*, and six new species of *Diaporthe*. Two species, *Gnomoniopsis rosae* and *Coniella quercicola* are new records for China.

Introduction

The *Diaporthales* is an important and species-rich ascomycetous order in the subclass *Diaporthomycetidae* (*Sordariomycetes*). Despite its cosmopolitan distribution and high diversity with distinctive morphology, this order has received relatively little attention. Currently the existing classification of the group reveals 31 accepted families within the order *Diaporthales* (Jiang et al. 2020), including *Foliocryphiaceae*, *Diaporthaceae*, *Gnomoniaceae* and *Schizoparmaceae*. Members of *Diaporthales* have a wide range of ecological habitats and numerous modes of nutrition (Barr 1978). Except for members of *Tirisporellaceae*, most taxa in *Diaporthales* occur in terrestrial habitats. Species in *Diaporthales* form solitary or aggregated, immersed to erumpent, rarely superficial, orange, brown or black perithecial ascomata, with short or long necks, that are located in stromatic tissues or substrates, with a hamathecium lacking or with few paraphyses (Alexopoulus and Mims 1978; Barr 1978; Hawksworth et al 1995; Castlebury et al. 2002). Asci are unitunicate with a conspicuous refractive ring (Hawksworth et al. 1995; Rossman et al. 2007). Ascospores are diverse in shape, size and colour. The asexual morphs of *Diaporthales* are generally coelomycetous (Rossman et al. 2007), producing acervuli, pycnidial or synnematal conidiomata, with or without a well developed stroma. Conidiogenesis is phialidic or rarely annellidic and conidia are usually unicellular or 1-septate (Rossman et al. 2007).

Foliocryphiaceae (*Diaporthales*) was established by Jiang et al. (2020) based on the type genus *Foliocryphia* (Cheewangkoon et al. 2009), and two allied genera, *Chrysofolia* (Crous et al. 2015) and *Neocryphonectria* (Jiang et al. 2020).

Chrysofolia and *Foliocryphia* were originally placed in the family *Cryphonectriaceae*, but were transferred to *Foliocryphiaceae* by Jiang et al. (2020). Species of *Chrysofolia* usually exude a yellow slimy mass of conidia from a globose pycnidium with immersed base. Only two species are listed in MycoBank (www.mycobank.org; accessed 8 Oct 2022), *Ch. colombiana* (Crous et al. 2015), a pathogen of *Eucalyptus urophylla* from Colombia, and *Ch. barringtoniae* (Suwannarach et al. 2016), an endophyte of *Barringtonia acutangula* from Thailand.

Diaporthe is a large genus in *Diaporthaceae*, with 1168 epithets listed in Index Fungorum (http://www.indexfungorum.org/; accessed 4 July 2022), but only one-fifth of these taxa have been studied with molecular data (Guo et al. 2020; Yang et al. 2020; Zapata et al. 2020). The sexual morph of *Diaporthe* is characterized by immersed perithecial ascomata and an erumpent pseudostroma with more or less elongated perithecial necks; unitunicate clavate to cylindrical asci; and fusoid, ellipsoid to cylindrical, septate

or aseptate, hyaline ascospores, biseriately to uniseriately arranged in the ascus, sometimes having appendages (Udayanga et al. 2011; Senanayake et al. 2017, 2018). The asexual morph is characterized by ostiolate conidiomata, with cylindrical phialides producing three types of hyaline, aseptate conidia (Udayanga et al. 2011; Gomes et al. 2013): type I α-conidia are hyaline, fusiform, straight, guttulate or eguttulate, aseptate, and smooth-walled; type II β-conidia are hyaline, filiform, straight or hamate, aseptate, smooth-walled, and eguttulate; while type III γ-conidia are rarely produced, and are hyaline, multiguttulate, fusiform to subcylindrical with an acute or rounded apex, while the base is sometimes truncate.

Gnomoniaceae is a large family within *Diaporthales*, containing 38 accepted genera (Mejía et al. 2011a, 2011b, 2012; Walker et al. 2012; Jiang and Tian 2019). Among them, *Gnomoniopsis* is a well delimited genus inhabiting leaves, branches and fruits of hosts in three families, *Fagaceae*, *Onagraceae* and *Rosaceae* (Sogonov et al. 2008; Walker et al. 2010; Jiang and Tian 2019; Yang et al. 2020). The sexual morph of *Gnomoniaceae* is characterized by ascomata that are generally immersed, solitary or aggregated in an undeveloped stroma (Rossman et al. 2007; Sogonov et al. 2008). The perithecia are dark brown to black and pseudoparenchymatous with central, eccentric, or lateral necks (Rossman et al. 2007; Sogonov et al. 2008). Asci usually have an inconspicuous or distinct apical ring. Ascospores are generally small, hyaline, and uniseptate. The asexual morph is characterized by acervular or pycnidial conidiomata, phialidic conidiogenous cells, and non-septate conidia (Monod 1983).

The family *Schizoparmeaceae* (*Diaporthales*) was introduced by Rossman et al. (2007). Historically, the family consisted of three genera, two of which only produce asexual morphs (*Coniella* and *Pilidiella*) and one that can produce sexual morphs (*Schizparme*) (Rossman et al. 2007). This family was reassessed by Alvarez et al. (2016), who proposed that *Pilidiella* is a taxonomic synonym of *Coniella*. *Coniella* was erected by Höhnel (1918) and typified by *C. pulchella*. (Petrak and Sydow 1927) separated the genus into *Euconiella* (with dark conidia) and *Pseudoconiella* (with pale conidia) (Alvarez et al. 2016). The key characters of *Coniella* are erumpent, brown or black ascomata or conidiomata that later become superficial, with an irregularly thickened peridium with plate-like ornamentation and one-celled ascospores, initially

hyaline and later becoming pale to dark brown (Senanayake et al. 2018).

Morphological comparisons and phylogenetic analyses have been commonly used to describe the taxa of *Diaporthales* and to confirm their taxonomic placement. The present study follows a recently revised classification (Jiang et al. 2020), combined with molecular and morphology and introduces some novel taxa within the family *Diaporthales* found in Guizhou, China. Genealogical Concordance Phylogenetic Species Recognition (GCPSR) was also used for delineation of *Foliocryphiaceae*, *Diaporthe*, *Gnomoniopsis* and *Coniella* species. GCPSR relies on performing a pairwise homoplasy index coupled with phylogenetic relatedness in a multi-locus dataset and the interpretation of nucleotide differences (Taylor et al. 2000; Huson and Bryant 2006).

Materials And Methods

Sample collection and fungal strain isolation

The plant samples were collected from Wengan, Longli and Dejiang counties, Guizhou Province, China. They were placed in envelopes, and taken back to the laboratory and photographed. Before single-spore isolation, the surface of the samples were disinfected by spraying 2 or 3 times with 75% ethanol . The single spore isolation procedure of Chomnunti et al. (2014) was followed in order to obtain pure cultures. Each pure culture was spread onto 90-mm diam. Petri dishes containing either potato dextrose agar (PDA) or oatmeal agar (OA) (Zhang et al. 2017). *Diaporthe* were induced to sporulate by plating them on 2 % water agar (WA) (Santos et al. 2017) containing sterilized pine needles. These dishes were cultured at a constant temperature (25 ºC) under a 12 h light/dark regime in a light incubator. Dried holotype specimens were conserved in the Herbarium of Department of Plant Pathology, Agricultural College, Guizhou University (HGUP). Ex-type cultures were conserved in the Culture Collection at the Department of Plant Pathology, Agriculture College, Guizhou University, P.R. China (GUCC).

Morphological description

The pure cultures were grown on PDA and OA media in a constant temperature incubator (25 °C) under a 12 h light/dark regime. Culture characteristics were recorded and examined using a stereo-microscope (LEICA S9i, Germany). Morphological observations were made with a Zeiss Scope 5 (Axioscope 5, China) equipped with an AxioCam 208 color camera (ZEN 3.0) and measurements were made with ZEN 3.0. Adobe Photoshop CC 2017 was used to make the photoplates. All new taxa were registered in MycoBank (Crous et al. 2004).

DNA extraction, PCR amplification and sequencing

Fresh mycelium was scraped from cultures using a sterilized scalpel and genomic DNA was extracted using Fungal gDNA Kit (Biomiga #GD2416, San Diego, California, USA) in accordance with the manufacturer's instructions. Five genes were selected: internal transcribed spacers (ITS), 28s subunit rDNA (LSU), RNA polymerase II subunit 2 (*rpb2*), translation elongation factor 1 (*tef1*), and β-tubulin gene region (*tub2*). Polymerase chain reactions (PCR) were carried out in 20 µL reaction volume, which contained 10 µL 2 × PCR Master Mix, 7 µL ddH_2O, 1 µL of each primer, 1 µL template DNA. The PCR thermal cycle program and primers are shown in Table 1. Purification and sequencing of PCR products were carried out by the Sangon Biotech Company (Shanghai, China).

Table 1. Primers and PCR procedures used in this study.

Locus	Primers	Primer sequence (5’–3’)	PCR thermal cycle protocals	References
ITS	ITS5	GGAAGTAAAAGTCGTAACAAGG	94°C–2 min; 94°C–1 min; 58°C–1 min; 72°C–90 sec; repeat 2–4 for 35 cycles; 72°C–10 min; 4°C on hold	White et al. (1990)
	ITS4	TCCTCCGCTTATTGATATGC		
LSU	LR0R	ACCCGCTGAACTTAAGC		Rehner and Samuels (1995); Vilgalys and Hester (1990)
	LR5	TCCTGAGGGAAACTTCG		
rpb2	fRPB2-5F	GAYGAYMGWGATCAYTTYGG	94°C–2 min; 95°C–45 sec; 57°C–50 sec; 72°C–90 sec; repeat 2–4 for 35 cycles; 72°C–10 min; 4°C on hold	Liu et al. (1999)
	fRPB2-7cR	CCCATRGCTTGYTTRCCCAT		
tef1	EF1-728F	CATCGAGAAGTTCGAGAAGG	94°C–2 min; 95°C–30 sec; 58°C–50 sec; 72°C–1 min; repeat 2–4 for 35 cycles; 72°C–10 min; 4°C on hold	Carbone and Kohn (1999)
	EF1-986R	TACTTGAAGGAACCCTTACC		
tub2	Bt2a	GGTAACCAAATCGGTGCTGCTTTC	95°C–5 min; 95°C–30 sec; 60°C–30 sec; 72°C–30 sec; repeat 2–4 for 34 cycles; 72°C–10 min; 4°C on hold	Glass and Donaldson (1995)
	Bt2b	ACCCTCAGTGTAGTGACCCTTGGC		

Phylogeny

Sequences used in this study (Tables 2–6) were assembled based on the closest matches from BLASTn search results (https://blast.ncbi.nlm.nih.gov/Blast.cgi) and previous publications (Maharachchikumbura et al. 2015, 2016; Senanayake et al. 2017, 2018; Crous et al. 2018; Guarnaccia et al. 2018; Raudabaugh et al. 2018; Hyde et al. 2020; Jiang et al. 2020; Tennakoon et al. 2021). Alignments were conducted with the online version of MAFFT v. 7.505 (Katoh and Standley 2016), checked visually and improved manually where necessary using BioEdit 7.1.3.0 (Hall 1999). Sequence matrix v. 1.7.8 (Vaidya et al. 2011) was used to concatenate the aligned sequences of the different loci. Ambiguous areas were excluded from the analysis using Aliview (Larsson 2014) and gaps were viewed as missing data. The final alignments were deposited in TreeBASE (www.treebase.org) under accession number 29787.

Phylogenetic analyses were carried out by maximum likelihood (ML), maximum parsimony (MP) and Bayesian inference (BI). The ML analysis was performed using RAxML-HPC BlackBox(8.2.12) (Stamatakis 2006) partial and general time reversible model (GTR) using the discrete gamma distribution as the evolution model by CIPRES Science Gateway version 3.3 (Miller et al. 2010). Non-parametric bootstrap analysis was implemented with 1000 iterations. The resulting duplicates were plotted on to the best scoring tree previously obtained.

Maximum parsimony (MP) analyses were performed with PAUP on XSEDE (4.a168) on CIPRES Science Gateway v. 3.3, using the heuristic search option with 1,000 random sequence addition replicates and tree bisection-reconnection (TBR) with reconnection limit (=8) as the branch swapping algorithm. Maxtrees was set at 5,000 (and not increased). Branches were collapsed creating polytomies if maximum branch length was zero. Tree length (TL), consistency index (CI), retention index (RI), rescaled consistency index (RC) and homoplasy index (HI) were calculated for each tree generated.

Bayesian inference (BI) analysis was performed by MrBayes 3.2.7a (Ronquist et al. 2012) in the CIPRES Science Gateway version 3.3. The optimal substitution model with gamma rates and dirichlet base frequencies for ITS, LSU, *rpb2*, *tef1* and *tub2* sequences were decided by modelGUI for each locus (Nylander 2004). The Markov chain Monte Carlo (MCMC) sampling approach was used to calculate posterior

probabilities (PP) (Rannala and Yang 1996). Six simultaneous Markov chains were run for 50 million generations and trees were sampled every 1000th generation; thus, 50,000 trees were obtained. The first 25% of trees, representing the burn-in phase of the analyses, were discarded and the remaining trees were used for calculating posterior probabilities (PP) in the majority rule consensus tree.

The phylogenetic trees were viewed with FigTree v. 1.4.3 (Rambaut 2016) and processed with Adobe Illustrator CS5. ML bootstrap support (MLBS) and MP bootstrap support (PBS) equal or greater than 70% (Hillis and Bull 1993) and Bayesian posterior probabilities (PP) equal or greater than 0.95 (Hespanhol et al. 2019), are displayed respectively in the first, second, and third positions on the edited phylogenetic tree.

Genealogical Phylogenetic Species Recognition (GCPSR) analysis

Morphologically and phylogenetically related species were analyzed using GCPSR as described by Taylor et al. (2000) by pairwise homogeneity index test (PHI) (Bruen et al. 2006). The PHI tests were performed in SplitsTree v. 4.17.1 (Huson 1998; Huson and Bryant, 2006) as described by Quaedvlieg et al. (2014) to determine the level of recombination within phylogenetically closely related species. This test determines the probability (P-value) of the null hypothesis of no recombination within the dataset. When the P-value is less than 0.05, we reject the null hypothesis and accept the alternate hypothesis that there is evidence for the presence of recombination. The results were visualized by constructing a split graph using LogDet conversion and the Splits options.

Results

Phylogenetic analyses

To reveal the phylogenetic position of family *Foliocryphiaceae*, genera *Diaporthe*, *Gnomoniopsis* and *Coniella* within the order *Diaporthales*, phylogenetic analyses were performed with ITS, LSU, *rpb2*, *tef1* and *tub2* sequence data.

The first sequences dataset of ITS, LSU, *rpb2*, *tef1* and *tub2* was analyzed to focus on *Foliocryphiaceae*. The alignment included 43 taxa, including the outgroup sequences of *Dwiroopa lythri* (CBS 109755, ex-type strain) and *Dw. punicae* (CBS 143163, ex-type strain) (Tables 2, 6). The aligned five-locus datasets comprised 3596 characters of family *Foliocryphiaceae*, viz. ITS: 1–769, LSU: 770–1617, *rpb2*: 1618–2442, *tef1*: 2443–2952 and *tub2*: 2953–3596. Of these, 2145 characters were constant, and 1131 characters were parsimony-informative and 320 were parsimony-uninformative (gaps treated as missing). The parameter settings used are shown in Table 7. The tree of RAxML was selected to show the topology (Fig. 1), and the MP and Bayesian analyses resulted in similar topology to ML.

Table 7. Parameters of maximum parsimony and Bayesian methods in this study.

Datasets	Maximum Parsimony (MP)					
	TL	PT	CI	RI	RC	HI
Foliocryphiaceae	4515	9	0.5132	0.6746	0.3462	0.4868
Diaporthe	2596	108	0.5177	0.8202	0.4246	0.4823
Gnomoniopsis	2423	3	0.5712	0.5930	0.3387	0.4288
Coniella	1292	8	0.5735	0.7112	0.4079	0.4265
	Bayesian					
	Model					ASDSF
	ITS	LSU	*rpb2*	*tef1*	*tub2*	
Foliocryphiaceae		GTR+I+G		HKY+I+G	HKY+G	0.009523
Diaporthe	SYM+I+G	n/a	n/a	HKY+I+G		0.009925
Gnomoniopsis	GTR+I+G	GTR+I	GTR+G	HKY+I+G	GTR+I+G	0.009908
Coniella	SYM+I+G	GTR+I+G	n/a	GTR+I+G	n/a	0.009408

TL: Tree length; PT: Parsimonious tree; CI: Consistency indices; RI: Retention indices; RC: Rescaled consistency indices; HI: Homoplasy index

Model: the best nucleotide substitution model used for the different partitions

ASDSF: average standard deviation of split frequencies

Two strains (GUCC 416.4, ex-type strain and GUCC 416.14) shared the same branch length with 100% MLBS/99% MPBS/1 PP support and grouped with the type strains of *Ch. colombiana* (CPC 24986) and *Ch. barringtoniae* (TBRC 5647) with high statistical support (76% MLBS/99% MPBS)/(100% MLBS/99% MPBS/1 PP) (Fig. 1), respectively. The comparison of DNA bases composition (Table 8) indicated that between our two strains and *Ch. colombiana* (CPC 24986), there were 7 bases different in the ITS region, 2 bases different in the LSU region, and 149 bases different in the *tef1* region. Between GUCC 416.4 and GUCC 416.14, and *Ch. barringtoniae* (TBRC 5647), there were 31 different bases in the ITS region, and 4 different bases in the LSU region. Unfortunately, *Ch. colombiana* did not have *rpb2* and *tub2* sequences data, and *Ch. barringtoniae* did not have *rpb2*, *tef1* and *tub2* sequences data.

Four strains (GUCC 406.6, ex-type strain, GUCC 405.3, GUCC 405.4 and GUCC 405.8) formed a stable subclade, clustered with the genera *Neocryphonectria*, *Chrysofolia*, and *Foliocryphia*. They formed a well-resolved clade (99% MLBS/94% MPBS/1 PP) within *Foliocryphiaceae*. Our four strains were closer to *N. carpini* (CFCC 53027, ex-type strain) and *N. chinensis* (CFCC 53025, ex-type strain and CFCC 53029) with high support in their respective branches (97% MLBS/1 PP) (Fig. 1). The comparison of DNA bases (Table 8) revealed 116/118/32 base pair difference in ITS, 22/21/21 base pair difference in LSU, no data and 75/76 base pair difference in *rpb2* and no data and 130/130 base pair difference in *tef1* between our four strains and *N. carpini* (CFCC 53027, ex-type strain) and *N. chinensis* (CFCC 53025, ex-type strain and CFCC 53029), but no *tub2* sequences data for comparison.

The pairwise homoplasy index (PHI) (Fig. 5a) test revealed that there was no significant recombination (P-value = 1.0) between our strains (GUCC 416.4, GUCC 416.14, GUCC 406.6, GUCC 405.3, GUCC 405.4 and GUCC 405.8) and three other genera in *Foliocryphiaceae* (*Chrysofolia*, *Foliocryphia* and *Neocryphonectria*).

The second sequences dataset of ITS, *tef1* and *tub2* was analyzed in combination to infer the interspecific relationships within *Diaporthe*. The alignment included 67 taxa, including the outgroup sequences of *Diaporthella corylina* (CBS 121124, ex-neotype strain) (Tables 3, 6). The aligned three-locus datasets

comprised 1797 characters of *Diaporthe*, viz. ITS: 1–636, *tef1*: 637–1144 and *tub2*: 1145–1797. Of these, 965 characters were constant, and 608 characters were parsimony-informative and 224 were parsimony-uninformative (gaps were treated as missing). The parameter settings that were used are shown in Table 7. The tree of RAxML was selected to show the topology (Fig. 2), and the MP and Bayesian analyses resulted in similar topology to ML.

Two strains (GUCC 422.16, ex-type strain and GUCC 422.161) had a close relationship to *D. chimonanthi* (HGUP191001, HGUP192087) and *D. caryae* (CFCC 52563, ex-epitype strain, PSCG520), supported by MLBS (98%), PBS (94%) and PP (1) and MLBS (100%), PBS (100%) and PP (1), respectively (Fig. 2). The comparison of DNA bases (Table 8) showed that our strains kept some distinction to *D. chimonanthi* (HGUP191001, HGUP192087) and *D. caryae* (CFCC 52563, ex-type strain, PSCG520) with 18/23 and 2/4 base pair difference in the ITS, no data and 6/6 base pair difference in the *tef1*, and 5/2 and 17/30 base pair difference in the *tub2*. The pairwise homoplasy index (PHI) test (Fig. 5b) revealed that there was no significant recombination (P-value = 0.5412) among these two strains (GUCC 422.16 and GUCC 422.161), to *D. chimonanthi* (HGUP191001, HGUP192087) and *D. caryae* (CFCC 52563, ex-epitype strain, PSCG520).

Strains GUCC 420.9 (ex-type strain) and GUCC 420.19 shared the same branch length with 100% MLBS/100% MPBS/1 PP support and grouped with the ex-type strains of *D. passiflorae* (CBS 132527, ex-type strain) and *D. malorum* (CAA734, ex-type strain, CAA740, CAA752) with high statistical support (100% MLBS/100% MPBS/1 PP) (Fig. 2). The comparison of DNA bases (Table 8) reveals 11/15 bp difference in ITS, 23/19 bp difference in *tef1* and 13/13 bp difference in *tub2* between the two strains and *D. passiflorae* and *D. malorum*. The PHI test (Fig. 5c) did not find statistically significant evidence for recombination (P-value = 1.0) between the strains (GUCC 420.9 and GUCC 420.19) and related taxa *D. passiflorae* (CBS 132527, ex-type strain) and *D. malorum* (CAA734, ex-type strain, CAA740, CAA752).

GUCC 421.2 (ex-type strain) and GUCC 421.21 have a close relationship with *D. eres* (CBS 138594 ex-type strain, CAA801) with high support (95% ML, 88% MP, 1 PP) and formed a well-resolved clade sister to *D. eres* and *D. cotoneastri* (CBS 439.82, ex-type strain). The comparison of DNA bases (Table 8) shows 4/3/7 bp difference in ITS, 6/7/5 bp difference in *tef1* and 6/7/13 bp difference in *tub2* between GUCC 421.2 and GUCC 421.21 and other three strains in the clade. Based on the PHI test (Fig. 5d) there was no significant recombination (P-value = 1.0) between our strains (GUCC 421.2 and GUCC 421.21) and the sister taxon *D. eres* (CBS 138594, ex-type strain and CAA801).

Strains GUCC 421.10 (ex-type strain) and GUCC 421.101 formed a highly supported subclade (80% ML, 89% MP, 1 PP) with *D. phragmitis* (CBS 138897, ex-type strain). There were 8 base pair difference in the ITS and 13 base pair difference in the *tub2*. Unfortunately, *D. phragmitis* (CBS 138897, ex-type strain) did not have *tef1* sequences data for comparison. The PHI test (Fig. 5e) did not find statistically significant evidence for recombination (P-value = 1.0) between our *Diaporthe* strains (GUCC 421.10, ex-type strain and GUCC 421.101) and related taxa *D. ellipicola* (CGMCC 3.17084, ex-type strain and CGMCC 3.17085) and *D. phragmitis* (CBS 138897, ex-type strain).

Three strains (GUCC 412.7, ex-type strain, GUCC 412.71 and GUCC 412.17) shared the same branch length with 100% MLBS/100% MPBS/1 PP support and clustered with *D. lithocarpus* (CGMCC 3.15175, ex-type

strain, CGMCC 3.151777) with high statistical support (70% MLBS/70% MPBS/1 PP) (Fig. 2). The comparison of DNA bases (Table 8) reveals 7/9 bp difference in ITS, 15/11 bp difference in *tef1* and 11 bp difference and no data in *tub2* between these three strains and *D. lithocarpus* (CGMCC 3.15175 and CGMCC 3.151777). The PHI test (Fig. 5f) did not find statistically significant evidence for recombination (P-value = 1.0) between our *Diaporthe* strains (GUCC 412.7, ex-type strain, GUCC 412.71 and GUCC 412.17) and related taxon *D. lithocarpus*.

Two strains (GUCC 414.4, ex-type strain and GUCC 414.41) formed a high support subclade (100% ML, 100% MP, 1.00 PP) with *D. caulivora* (CBS 127268, ex-type strain, Dip1, Dpc11). There were 17 base pair difference in the ITS, 30 base pair difference in *tef1* and 11 base pair difference in the *tub2* from our strains by comparison of DNA bases (Table 8). The PHI test (Fig. 5g) did not find any statistically significant evidence for recombination (P-value = 1.0) between our two strains (GUCC 414.4, GUCC 414.41) and strains of *D. caulivora*.

The third sequences dataset of ITS, LSU, *rpb2*, *tef1* and *tub2* was analyzed in combination to infer the interspecific relationships within *Gnomoniopsis*. The alignment included 29 taxa, including the outgroup sequences of *Sirococcus tsugae* (CBS 119626) (Tables 4, 6). The aligned five-locus datasets comprised of 3354 characters of *Gnomoniopsis*, viz. ITS: 1–572, LSU: 573–1423, *rpb2*: 1424–2460, *tef1*: 2461–2861 and *tub2*: 2862–3354. Of these, 2431 characters were constant, and 615 characters were parsimony-informative and 308 were parsimony-uninformative (gaps are treated as missing). The parameter settings that were used are shown in Table 7. The tree of RAxML was selected to show the topology (Fig. 3), and the MP and Bayesian analyses resulted in similar topology to RAxML.

Our strains (GUCC 408.7 and GUCC 408.17) clustered in the same subclade (100% ML, 100% MP, 1.00 PP) with *G. rosae* (CBS 145085), and there were identical sequences in the ITS, LSU and *rpb2* regions. The phi test result (P-value = 1.0) (Fig. 5h) of our strains (GUCC 408.7 and GUCC 408.17), *G. rosae* (CBS 145085), *G. angolensis* (CBS 145057) and *G. clavulata* (AR 4313) showed no statistically significant recombination.

The fourth sequences dataset of ITS, LSU and *tef1* was analyzed in combination to infer the interspecific relationships within *Coniella*. The alignment included 32 taxa, including the outgroup sequences of *C. fragariae* (CBS 172.49, ex-type strain) and *C. nigra* (CBS 165.60, ex-type strain) (Tables 5, 6). The aligned three-locus datasets comprised of 2165 characters of *Coniella*, viz. ITS: 1–595, LSU: 596–1767 and *tef1*: 1768–2165. Of these, 1717 characters were constant, and 385 characters were parsimony-informative and 63 were parsimony-uninformative (gaps are treated as missing). The parameter settings that were used are shown in Table 7. The tree of RAxML was selected to show the topology (Fig. 4), and the MP and Bayesian analyses resulted in similar topology to RAxML.

Strains GUCC 414.2, GUCC 414.21, GUCC 412.3, GUCC 405.6 and GUCC 405.16 clustered very close to *C. quercicola* (CBS 904.69, ex-type strain, CBS 283.76 and CPC 12133) with only MP support (95% MPBS) (Fig. 4). The comparison of DNA bases composition (Table 8) indicated that between *C. quercicola* (CBS 904.69, ex-type strain, CBS 283.76 and CPC 12133) and our five strains (GUCC 414.2, GUCC 414.21, GUCC 412.3, GUCC 405.6 and GUCC 405.16), there were identical sequences in the ITS and LSU regions, but 1/5/10/10/18/7/6 bases different in the *tef1* region. The PHI test (Fig. 5i) did not find statistically significant

evidence for recombination (P-value = 0.2264) between our five strains and related taxa *C. quercicola* (CBS 904.69, ex-type strain, CBS 283.76 and CPC 12133).

Taxonomy

In this section, we introduce one new genus, eight new species and two new host and country records.

Pseudomastigosporella S.Y. Wang, Yong Wang bis & Y. Li, **gen. nov.**

MycoBank Number: MB846026

Etymology: In reference to *Mastigosporella*, to which this genus is morphologically similar.

Classification: Foliocryphiaceae, *Diaporthales*, *Sordariomycetes*.

Description: *Asexual morph*: *Conidiomata* pycnidial, globose or subglobose, base immersed, separate to aggregated, *mycelium* superficial, fluffy, granular, white or gray-white to pale yellow, exuding light brown-orange to medium brown-orange to deep brown-orange conidial masses, bright yellow or light orange in lactic acid, 2–5 wall layers of olive to gray-green textura angularis. *Conidiophores* reduced to conidiogenous cells. *Conidiogenous cells* arising from base, central cushion of hyaline cells, densely aggregated, slightly thicker, cylindrical to ampulliform, simple, lining the inner cavity of base, mostly hyaline, sometimes pale olive, smooth, cylindrical to ampulliform, straight to curved, sometimes wider at the base. *Conidia* solitary, hyaline, smooth, guttulate, fusoid to ellipsoidal, sometimes long bubble-shaped, straight to curved, aseptate, base tapering with flattened scar, apex with 1 tubular appendage. *Sexual morph:* Unknown.

Type species: *Pseudomastigosporella guizhouensis* S.Y. Wang, Yong Wang bis & Y. Li

Notes: In *Foliocryphiaceae*, the important morphological characters of asexual morph is to produce dimorphic conidia. The microconidia are minute, cylindrical, aseptate, hyaline to pale brown; macroconidia are fusoid, aseptate, hyaline (Jiang et al. 2020). However, *Pseudomastigosporella* only has macroconidia but like species in *Mastigosporellaceae* it has an apical appendage developing as continuation of conidium body. This feature may contradict the root of “key to genera in *Cryphonectriaceae*, *Foliocryphiaceae*, and *Mastigosporellaceae*” provided by Jiang et al. (2020). However, following our phylogenetic analyses we still propose that *Pseudomastigosporella* should be placed in *Foliocryphiaceae.*

Pseudomastigosporella guizhouensis S.Y. Wang, Yong Wang bis & Y. Li, **sp. nov.**

Fig. 6

MycoBank Number: MB846027

Etymology: In reference to the fungus being isolated from Guizhou Province.

Type: **China:** Guizhou Province: Wengan county, on leaves of *Hypericum patulum* and *Acer palmatum*, June 2021, S.Y. Wang (HGUP 406, holotype; HGUP 405, ex-type living culture GUCC 406.6).

Additional living cultures: GUCC 405.3, GUCC 405.4, GUCC 405.8.

Description: *Asexual morph*: *Conidiomata* pycnidial, globose or subglobose, base immersed, separate to aggregated, *mycelium* superficial, fluffy, granular, white or gray-white to pale yellow, producing light brown-orange to medium brown-orange to deep brown-orange conidial masses, up to 570 µm diam., bright yellow or light orange in lactic acid, 2–5 wall layers of olive to gray-green textura angularis, 50–570 µm diam. *Conidiophores* reduced to conidiogenous cells. *Conidiogenous cells* arising from base, central cushion of hyaline cells, densely aggregated, slightly thicker, cylindrical to ampulliform, simple, lining the inner cavity of base, mostly hyaline, sometimes pale olive, smooth, cylindrical to ampulliform, straight to curved, sometimes wider at the base, 5–20 × 1.5–4.5 µm ($\bar{x}$ = 12 × 3 µm; n = 20). *Conidia* solitary, hyaline, smooth, guttulate, fusoid to ellipsoidal or fish-shaped, sometimes long bubble-shaped, straight to curved, aseptate, 15–31 × (3.5–)5.5–8.5 µm ($\bar{x}$ = 25 × 6.5 µm; n = 30), base tapering with flattened scar, 1.5–4 µm diam., with 1 apical, tubular appendage, 3.5–14.5 µm long. *Sexual morph:* Unknown.

Culture characteristics: Colonies covering 9 cm Petri dish after 2 weeks at 25 °C and a 12 h light/dark regime. On PDA, white or gray-white, fluffy, granular, effuse surface, reverse white or beige; on OA, white or gray-white to pale yellow, fluffy, granular, effuse surface, exuding light brown-orange to medium brown-orange to deep brown-orange conidial masses, reverse white or beige to pale yellow.

Notes: Although *Ps. guizhouensis* produces macroconidia with 1 tubular apical appendage, the conidia of this species differs in shape and size from those of C*hrysofolia* and *Foliocryphia.* The conidia of C*hrysofolia* are ellipsoidal and measure (4–)6–7.5(–10) × (2–)2.5(–3) µm (Crous et al. 2015) while those of *Foliocryphia* are also ellipsoidal and measure (5–)6–8(–9) × (2–)2.5(–3) µm (Cheewangkoon et al. 2009). Phylogenetically, our four *Pseudomastigosporella* strains reside within the *Foliocryphiaceae* clade, but appear not to fit into any presently circumscribed genus. The results of DNA base comparisons (Table 8) showed that there were striking differences in each gene between our four *Pseudomastigosporella* strains and adjacent genera. Based on distinct morphological characteristics, DNA phylogeny, DNA base differences and pairwise homoplasy index (PHI) test result, *Pseudomastigosporella* is described here as a new genus in *Foliocryphiaceae* with *Ps. guizhouensis* as the type species.

Chrysofolia coriariae S.Y. Wang, Yong Wang bis & Y. Li, **sp. nov.**

Fig. 7

MycoBank Number: MB845958

Etymology: In reference to the plant *Coriaria nepalensis*, from which this fungus was collected.

Type: **China:** Guizhou Province: Longli county, on leaves of *Coriaria nepalensis*, June 2021, S.Y. Wang (HGUP 416, holotype; ex-type living culture GUCC 416.4). *Additional living culture*: GUCC 416.14).

Description: Asexual morph: Conidiomata pycnidial, globose or subglobose, separate to aggregated, *mycelium* superficial and immersed, exuding yellow to bright orange to brown orange wet conidial masses, green-brown in lactic acid, but bright yellow or light orange in sterile water, 2–6 wall layers of green-brown to

brown textura angularis, 50–400 µm diam.; neck 15–60 µm long, 50–200 µm diam. where attached to the globose, terminating in an obtusely rounded apex. *Conidiophores* reduced to conidiogenous cells. *Conidiogenous cells* arising from base, central cushion of hyaline cells, densely aggregated, slightly thicker, tapering or cylindrical to ampulliform, simple, lining the inner cavity of base, hyaline, smooth, cylindrical to ampulliform, straight to curved, wider at the base, 5–20 × 1–3.5 µm. *Conidia* solitary, hyaline, smooth, ellipsoidal, or crescent-shaped, straight to allantoid, apex obtuse, base tapering with flattened scar, 0.5 µm diam., 5.5–9 × 2–4 µm ($\bar{x}$ = 7 × 2.7 µm; n = 30). *Sexual morph:* Unknown.

Culture characteristics: Colonies culturing under a controlled temperature light incubator at 25°C and a 12 h light/dark regime for 2 weeks. *Colonies* on PDA 75–90 mm diam. after 2 weeks at 25°C, light brown to white or gray-white, felty, effuse surface, with white fluffy even mycelium margin, reverse brown to light brown to white edge. *Colonies* on OA 65–85 mm diam. after 2 weeks at 25°C, light brown to white or gray-white, flat surface, exuding orange or brown conidial masses, reverse light brown to white or gray-white.

Notes: Conidiogenous cells of *Ch. coriariae* (5–20 × 1–3.5 µm) are longer than those of *Ch. colombina* (5–8 × 2–3 µm) (Crous et al. 2015) and *Ch. barringtoniae* (3–7.5 × 2–3 µm) (Suwannarach et al. 2016) and the conidiomata of *Ch. coriariae* (5–400 µm) are larger than those of *Ch. barringtoniae* (5–110 µm) (Suwannarach et al. 2016). *Chrysofolia coriariae* is phylogenetically distinct from other known species (Fig. 1). *Chrysofolia coriariae* has some differences in DNA base comparison with *Ch. colombina* and *Ch. barringtoniae* (Table 8). The new isolates are described here as a new species based on its distinct morphological characteristics, DNA phylogeny, DNA base differences and pairwise homoplasy index (PHI) test result.

Diaporthe juglandigena S.Y. Wang, Yong Wang bis & Y. Li, **sp. nov.**

Fig. 8

MycoBank Number: MB845959.

Etymology: Name refers to the plant host genus (*Juglans*) from which this fungus was collected.

Type: **China:** Guizhou Province: Dejiang County, on the peel of *Juglans regia*, September 2021, S.Y. Wang (HGUP 422, holotype; ex-type living culture GUCC 422.16).

Additional living culture: GUCC 422.161.

Description: Asexual morph: Conidiomata pycnidial, scattered, immersed or superficial, irregular globose and subglobose to slightly erumpent, black conidial masses surrounded by white mycelium, up to 2 mm diam, exuding transparent drops of water. *Conidiophores* reduced to conidiogenous cells. *Conidiogenous cells* densely aggregated, slightly thicker, subulate, simple, rarely branched above, simple, tapering, hyaline, smooth, 19–34 × 1–2.5 µm ($\bar{x}$ = 27 × 1.7 µm; n = 20), wider at base, rarely branched, densely aggregated, cylindrical, straight to sinuous. *Alpha conidia* hyaline, fusoid to ellipsoidal, asymmetrical, frequently guttulate, smooth-walled, 0–1-septate, tapering towards both ends, mostly straight, 5–8 × 2–3 µm ($\bar{x}$ = 6.4 ×

2.3 µm; n = 30). *Beta conidia* infrequent, hyaline, filiform, aseptate, smooth, eguttulate, apex acute, mostly curved, 23–36 × 1–2 µm ($\bar{x}$ = 31 × 1.3 µm; n = 10). *Gamma conidia* not observed. *Sexual morph:* Not observed.

Culture characteristics: Colonies covering 9 cm Petri dish after 2 weeks at 25 °C and a 12 h light/dark regime; spreading with uneven aerial *mycelium*. On PDA, surface with abundant aerial mycelium, white or gray-white to pale brown; reverse white to pale yellow to light brown. On OA surface with white or pale white to pale yellow thin aerial mycelium, with black conidial masses surrounded by white or gray-white mycelium; reverse white or beige to light yellow. On pine needles, irregular dark green to black subglobose conidial masses surrounded by thick white mycelium.

Notes: Conidiomata of *D. juglandigena* (2 mm diam) are larger than those of *D. chimonanthi* (= *Phomopsis chimonanthi*) (150–238 µm wide, 130–230 µm high) (Chang et al. 2005) and *D. caryae* (310–325 µm diam.) (Yang et al. 2018b). Conidiogenous cells and beta conidia of *D. juglandigena* (19–34 × 1–2.5 µm, 23–36 × 1–2 µm) are longer than those of *Phomopsis chimonanthi* (13–25 × 1.6–2.5 µm, 15–18 × 1–1.5 µm) and *D. caryae* (7–11 × 1.4–2.2 µm,15–34 × 1.1–1.4 µm), while the alpha conidia of *D. juglandigena* (5–8 × 2–3 µm) are shorter than those of *P. chimonanthi* (6.6–8.8 × 1.8–2.2 µm) and *D. caryae* (7–8.5 × 2.1–2.5 µm). *Diaporthe juglandigena* is phylogenetically distinct from the species presently known from DNA analyses (Fig. 2). The results of DNA base comparisons (Table 8) showed that there were significant differences in three loci between our two *D. juglandigena* strains and sister species (*D. chimonanthi* and *D. caryae*). Based on its distinct morphological characteristics, DNA phylogeny, DNA base differences and pairwise homoplasy index (PHI) test results, *D. juglandigena* is described here as a new species.

Diaporthe eucommiigena S.Y. Wang, Yong Wang bis & Y. Li, **sp. nov.**

Fig. 9

MycoBank Number: MB845961.

Etymology: eucommiigena, in reference to plant host (*Eucommia ulmoides*), from which the fungus was isolated.

Type: **China:** Guizhou Province: Guiyang: Huaxi district, South Campus of Guizhou University, on dead wood of *Eucommia ulmoides*, March 2022, S.Y. Wang (HGUP 420, holotype; ex-type living culture GUCC 420.9).

Additional living culture: GUCC 420.19.

Description: Asexual morph: Conidiomata pycnidial, separated but sometimes aggregated, immersed, sometimes superficial, irregular globose or subglobose, formimg dark olive or dull green to black conidial masses, up to 2 mm diam., sometimes surrounded by white mycelium. *Conidiophores* reduced to conidiogenous cells. *Conidiogenous cells* densely aggregated, slightly thicker, subulate, hyaline, simple, rarely branched above, simple, hyaline, smooth, 12–27.5 × 1.5–3 µm ($\bar{x}$ = 19 × 2.2 µm; n = 20), wider at base, tapering at apex, rarely branched, densely aggregated, cylindrical, slightly bent. *Alpha conidia* hyaline, fusoid

to ellipsoidal, frequently guttulate, asymmetrical, smooth-walled, 0–1-septate, tapering towards both ends, mostly straight, 5.5–8 × 1.5–3 µm ($\bar{x}$ = 7 × 2.3 µm; n = 30). *Beta conidia* hyaline, filiform, aseptate, smooth, eguttulate, apex acute, mostly curved, 27–37 × 1–2 µm ($\bar{x}$ = 32 × 1.3 µm; n = 10). *Gamma conidia* hyaline, fusoid to ellipsoidal, frequently guttulate, smooth, aseptate, straight, tapering at apex, 7.5–10 × 1.5–2.5 µm ($\bar{x}$ = 8.6 × 2.1 µm; n = 20). *Sexual morph:* Not observed.

Culture characteristics: Colonies covering 9 cm Petri dish after 2 weeks at 25 °C and a 12 h light/dark regime; spreading with uneven aerial *mycelium*. On PDA, surface with abundant white to pale yellow, uneven zonated aerial mycelium and margin, distinctly imbricated like a flower; reverse with pale yellow to light brown and pale pink, uneven zonated aerial mycelium and margin, exuding abundant dark green to black spots with age. On OA surface with uneven white to olive aerial mycelium, forming black conidial masses surrounded by white or gray-white mycelium; reverse white to olive, irregular. On pine needles, irregular dark green to black subglobose conidial masses surrounded by thick gray-white mycelium.

Notes: Conidiomata of *Diaporthe eucommiigena* (2 mm diam.) are larger than those of *D. passiflorae* (300 µm diam.) (Crous et al. 2012). Conidiogenous cells of *D. passiflorae* are 2–3-septate, while those of *D. eucommiigena* are aseptate; conidiogenous cells of *D. eucommiigena* (12–27.5 × 1.5–3 µm) are smaller than those of *D. passiflorae* (20–30 × 2.5–4 µm) while beta conidia of *D. eucommiigena* (27–37 × 1–2 µm) are longer than *D. passiflorae* (14–20 × 1.5–2 µm) and *D. malorum* (17.4–26.6 × 0.8–2 µm) (Santos et al. 2017). Gamma conidia were not observed in *D. passiflorae* but are present in *D. eucommiigena*. *Diaporthe eucommiigena* is phylogenetically distinct from the species presently known from DNA data (Fig. 2). The comparison of DNA bases (Table 8) showed significant difference between *D. eucommiigena* and adjacent species (*D. passiflorae* and *D. malorum*). Based on distinct morphological characteristics, DNA phylogeny, DNA base differences and pairwise homoplasy index (PHI) test results, *D. eucommiigena* is described here as a new species.

Diaporthe dejiangensis S.Y. Wang, Y. Wang bis & Y. Li, **sp. nov.**

Fig. 10

MycoBank Number: MB845962.

Etymology: Name refers to the location (Dejing), from where the host plant was collected.

Type: **China:** Guizhou Province: Dejiang County, on the peel of *Juglans regia*, September 2021, S.Y. Wang (HGUP 421, holotype; ex-type living culture GUCC 421.2).

Additional living culture: GUCC 421.21.

Description: Asexual morph: Conidiomata pycnidial, soliary to aggregated, immersed or superficial, irregular globose or subglobose to depressed, exuding white to dark brown to black conidial masses, with age surrounded by thin white mycelium, up to 2 mm diam., 4–7 wall layers of olive textura angularis. *Conidiophores* reduced to conidiogenous cells. *Conidiogenous cells* densely aggregated, hyaline, smooth,

cylindrical, wider at base, mostly straight, phialidic, simple, subcylindrical, tapering towards apex, hyaline, smooth, 9.5–17 × 1–3 µm ($\bar{x}$ = 13 × 1.8 µm; n = 30), mostly straight, rarely branched. *Alpha conidia* hyaline, fusiform to ellipsoidal, frequently guttulate, asymmetrical, smooth-walled, 0–1-septate, rounded towards both ends, mostly straight, 6–8.5 × 1.5–3 µm ($\bar{x}$ = 7 × 2.3 µm; n = 30). *Beta conidia* and *gamma conidia* not observed. *Sexual morph:* Not observed.

Culture characteristics: Colonies covering 9 cm diam. Petri dish after 2 weeks at 25 °C and a 12 h light/dark regime. On PDA surface with thick aerial mycelium, flat, velvet, white and beige; reverse white to pale yellow. On OA surface with white or pale white thin aerial mycelium, exuding black conidial masses, surrounded by white mycelium; reverse white or beige. On pine needles, irregular, black, globose conidial masses surrounded by thick white mycelium.

Notes: Conidiomata of *D. dejiangensis* (2 mm diam.) are larger than those of *D. cotoneastri* (1.5 mm diam.) (Udayanga et al. 2012), while its alpha conidia (6–8.5 × 1.5–3 µm) are smaller than those of *D. cotoneastri* (6–10 × 2–3 µm). Neither beta nor gamma conidia were observed for *D. dejiangensis,* while *D. cotoneastri* produced beta conidia (18–25 × 1 µm). *Diaporthe dejiangensis* is phylogenetically distinct from the species presently known from DNA data (Fig. 2). The results of DNA base comparisons are shown in Table 8, and there are many base differences among three genes. Based on its distinct morphological characteristics, DNA phylogeny, DNA base differences and pairwise homoplasy index (PHI) test results, *D. dejiangensis* is described here as a new species.

Diaporthe tongrensis S.Y. Wang, Yong Wang bis & Y. Li, **sp. nov.**

Fig. 11

MycoBank Number: MB845963.

Etymology: tongrensis, in reference to the city (Tongren), where the fungus was isolated.

Type: **China:** Guizhou Province: Tongren City, Dejiang County, on the peel of *Juglans regia*, September 2021, S.Y. Wang (HGUP 421, holotype; ex-type living culture GUCC 421.10).

Additional living culture: GUCC 421.101.

Description: Asexual morph: Conidiomata pycnidial, separated, immersed or superficial, irregular globose or subglobose to depressed, exuding black conidial masses surrounded by white mycelium, up to 2.5 mm diam., 7–10 wall layers of olive textura angularis. *Conidiophores* reduced to conidiogenous cells. *Conidiogenous cells* densely aggregated, slightly thicker, subulate, simple, rarely branched above, tapering, hyaline, smooth, 12–24 × 1.5–2.5 µm ($\bar{x}$ = 16 × 1.8 µm; n = 20), wider at base, cylindrical, straight to sinuous. *Alpha conidia* hyaline, fusoid to ellipsoidal, asymmetrical, smooth-walled, 1-septate, rounded towards both ends, mostly straight, 5.5–7.5 × 2–3 µm ($\bar{x}$ = 6.5 × 2.5 µm; n = 30). *Beta conidia* infrequent, hyaline, filiform, aseptate, eguttulate, smooth, apex acute, base slightly truncate, mostly straight, sometimes curved, 20–30 × 1–2 µm ($\bar{x}$ = 25.5 × 1.5 µm; n = 15). *Gamma conidia* not observed. *Sexual morph:* Not observed.

Culture characteristics: Colonies covering 9 cm diam. Petri dish after 2 weeks at 25 °C and a 12 h light/dark regime; spreading with aerial mycelium and uneven zonation. On PDA, surface with abundant aerial mycelium, with white uneven zonated aerial mycelium in the middle; reverse with white to pale yellow to light brown, uneven zonated aerial mycelium. On OA, surface with white or pale white, thin aerial *mycelium*, exuding black conidial masses surrounded by white mycelium; reverse white or beige. On pine needles, irregular black subglobose conidial masses surrounded by white mycelium.

Notes: Conidiomata of *D. tongrensis* (2.5 mm diam.) are larger than those of *D. phragmitis* (250 µm diam.) (Crous et al. 2014), and its conidiogenous cells are aseptate while those of *D. phragmitis* are 1–3-septate. The conidiogenous cells of *D. tongrensis* (12–24 × 1.5–2.5 µm) are smaller than those of *D. phragmitis* (20–30 × 3–4 µm). Alpha conidia of *D. tongrensis* (5.5–7.5 × 2–3) are shorter than those of *D. phragmitis* (7–8 × 2–3 µm). *Diaporthe tongrensis* formed beta conidia while neither beta nor gamma conidia were observed in *D. phragmitis*. *Diaporthe tongrensis* is phylogenetically distinct from the presently known species from DNA data (Fig. 2). *D. tongrensis* had some differences in DNA base comparison with *D. phragmitis*, shown in Table 8. Based on its distinct morphological characteristics, DNA phylogeny and DNA base differences, *D. tongrensis* is described here as a new species. *Diaporthe tongrensis* was described as a new taxon based on the high phylogenetic support for the clade, distinct morphological characteristics, DNA phylogeny, DNA base differences and pairwise homoplasy index (PHI) test results with adjacent species.

Diaporthe araliae-chinensis S.Y. Wang, Yong Wang bis & Y. Li, **sp. nov.**

Fig. 12

MycoBank Number: MB845964.

Etymology: In reference to the host plant, *Aralia chinensis*, from which this fungus was collected.

Type: **China:** Guizhou Province: Longli county, on leaves of *Aralia chinensis*, June 2021, S.Y. Wang (HGUP 412, holotype; ex-type living culture GUCC 412.7).

Additional living cultures: GUCC 412.17 and GUCC 412.71.

Description: Asexual morph: Conidiomata pycnidial, separated or aggregated, immersed or superficial, globose or subglobose, deep green to black, up to 1 mm diam., 5–8 wall layers of olive-green textura angularis. *Conidiophores* reduced to conidiogenous cells. *Conidiogenous cells* densely aggregated, smooth, cylindrical, subulate, mostly straight, phialidic, simple, cylindrical, hyaline, 12–20 × 1.5–2.5 µm ($\bar{x}$ = 16.5 × 2 µm; n = 20), slight taper towards apex, apex with inconspicuous periclinal thickening. *Alpha conidia* hyaline, fusoid to ellipsoidal, asymmetrical, smooth-walled, aseptate, tapering towards both ends, mostly straight, 5.5–9.5 × 2–3 µm ($\bar{x}$ = 7.5 × 2.4 µm; n = 30). *Beta conidia* and *gamma conidia* not observed. *Sexual morph:* Not observed.

Culture characteristics: Colonies covering 9 cm diam. Petri dish after 2 weeks at 25 °C and a 12 h light/dark regime. On PDA, surface with thick aerial mycelium, initially appearing white and light yellow becoming chartreuse or olive from the centre with age; reverse white to pale yellow to light olive. On OA, surface with

white or pale white thin aerial mycelium, exuding dark green to black conidial masses; reverse white or beige. On pine needles, irregular black conidial masses surrounded by sparse white mycelium.

Notes: Conidiomata of *D. araliae-chinensis* (1 mm diam.) are larger than those of *Phomopsis lithocarpius* (120–270 µm diam.) (Gao et al. 2014), while its conidiogenous cells and alpha conidia (12–20 × 1.5–2.5 µm, 5.5–9.5 × 2–3 µm) are longer than those of *P. lithocarpius* (12–15.4 × 1.9–2.6 µm, 5.7–8.1 × 2.1–3.2 µm). *Diaporthe araliae-chinensis* did not form beta and gamma conidia, while beta conidia of *P. lithocarpius* were 17.6–28.1 × 0.92–1.81 µm. *Diaporthe araliae-chinensis* is phylogenetically distinct from the species presently known from DNA data (Fig. 2). *Diaporthe araliae-chinensis* has some differences in DNA base comparison with *P. lithocarpius*, shown in Table 8. Based on its distinct morphological characteristics, DNA phylogeny, DNA base differences and pairwise homoplasy index (PHI) test results, *D. araliae-chinensis* is described here as a new species.

Diaporthe hyperici S.Y. Wang, Yong Wang bis & Y. Li, **sp. nov.**

Fig. 13

MycoBank Number: MB845965.

Etymology: Name refers to *Hypericum patulum*, the host genus from which this fungus was collected.

Type: **China:** Guizhou Province: Longli County, on leaves of *Hypericum patulum*, June 2021, S.Y. Wang (HGUP 416, holotype; ex-type living culture GUCC 416.4).

Additional living culture: GUCC 416.14.

Description: Asexual morph: Conidiomata pycnidial, separated or aggregated, immersed or superficial, globose or subglobose, deep brown to black, exuding black droplets from central ostioles with age, up to 3 mm diam., 6–10 wall layers of brown-green or brown textura angularis. *Conidiophores* reduced to conidiogenous cells. *Conidiogenous cells* densely aggregated, smooth, cylindrical, subulate, straight, phialidic, simple, cylindrical, hyaline, smooth, 11–21 × 1–3 µm ($\bar{x}$ = 17 × 1.9 µm; n = 30), slightly tapered towards apex, apex with inconspicuous periclinal thickening. *Alpha conidia* hyaline, fusoid to ellipsoidal, asymmetrical, smooth-walled, 0–1-septate, tapering towards both ends, mostly straight, 5–9.5 × 1.5–3 µm ($\bar{x}$ = 7 × 2.2 µm; n = 30). *Beta conidia* hyaline, spindle-shaped, aseptate, smooth, apex subacutate, base slightly truncate, sometimes straight, mostly curved, 10–20 × 1–2.5 µm ($\bar{x}$ = 15 × 1.5 µm; n = 30). *Gamma conidia* not observed. *Sexual morph:* Not observed.

Culture characteristics: Colonies covering 9 cm diam. Petri dish after 2 weeks at 25 °C and a 12 h light/dark regime. On PDA, surface with thick, white uneven zonated aerial mycelium, exuding brown to dark orange conidial masses; reverse white to pale yellow to light brown, uneven zonated aerial *mycelium* and margin. On OA, surface with white or gray-white to pale yellow, fluffy, granular aerial mycelium, exuding white to dark green to black conidial masses; reverse white or beige to pale yellow.

Notes: Conidiomata of *D. hyperici* (3 mm diam.) are larger than those of *D. caulivora* (230–310 µm diam.) (Santos et al. 2011), but the alpha conidia of *D. hyperici* (5–9.5 × 1.5–3 µm) are shorter than those of *D. caulivora* (8.9–9.2 × 2.4–2.5 µm). *Diaporthe caulivora* produce a sexual morph with unitunicate asci, while *D. hyperici* has no knonw sexual morph. *Diaporthe hyperici* is phylogenetically distinct from the presently known species from DNA data (Fig. 2). The comparison of DNA bases (Table 8) showed significant difference between *D. hyperici* and sister species (*D. caulivora*). Based on its distinct morphological characteristics, DNA phylogeny, DNA base differences and pairwise homoplasy index (PHI) test results, *D. hyperici* is described here as a new species.

Gnomoniopsis rosae Crous, Persoonia 41: 305 (2018)

MycoBank Number: MB 828203

Fig. 14

Materials examined: **China**: Guizhou Province: Wengan County, on leaves of *Rosa* sp. (*Rosaceae*), June 2021, S.Y. Wang (HGUP 408, living cultures GUCC 408.7 and GUCC 408.17) (**new country record**).

Description: Asexual morph: Conidiomata erumpent, separated, immersed or superficial, globose to depressed, initially appearing deep brown to black, slowly oozing transparent white or pale yellow oily spheres with age, up to 600 µm diam., 5–7 wall layers of olive brown to brown textura angularis. *Conidiophores* reduced to conidiogenous cells. *Conidiogenous cells* lining the inner cavity, hyaline, smooth, subcylindrical, branched at base or not, frequently branched above, simple, tapering, hyaline, smooth, subcylindrical, tapering towards apex, 6–15 × 1–3.5 µm ($\bar{x}$ = 11 × 2 µm; n = 20). *Conidia* solitary, aseptate, fusoid, hyaline, asymmetrical, guttulate, smooth-walled, rounded to acute apex, 6–12 × 2–4 µm ($\bar{x}$ = 8.5 × 3 µm; n = 30). *Sexual morph:* Unknown.

Culture characteristics: Colonies cultured at 25°C and a 12 h light/dark regime for 2 weeks on PDA 60–85 mm diam., forming a circle of transparent mycelium in the center, followed by a circle of white or gray-white thick ridges, then uneven zonated aerial mycelium, slightly imbricated, thick, initially appearing white to pale yellow, slowly turning olive-gray with age outside the two concentric rings, with an uneven edge; reverse transparent to white or olive and white uneven imbricated zonated to white or light brown uneven edge. *Colonies* on OA covering the whole dish, pale white or light gray-white, flat surface, exuding deep brown to black conidial masses, slowly oozing transparent white or pale yellow oily spheres with age, reverse pale white or light gray-white.

Notes: Gnomoniopsis represents a genus of mostly host specific fungi (Sogonov et al. 2008; Walker et al. 2010). *Gnomoniopsis rosae* (GUCC 408.7 and GUCC 408.17) is phylogenetically identical with the ex-type strain (CBS 145085) isolated by Crous et al. (2018) in ITS, LSU and *rpb2*, and we also supplemented the DNA sequences of this species with *tef1* and *tub2* genes. The DNA base comparison result is shown in Table 8, and there are no DNA base differences among several genes. The new isolates of *G. rosae* represent as a new record for China, based on morphological characteristics, DNA phylogeny, DNA base differences and pairwise homoplasy index (PHI) test results.

Coniella quercicola (Oudem.) L.V. Alvarez & Crous, Studies in Mycology 85: 27 (2016)

MycoBank Number: MB 817831

Fig. 15

Materials examined: **China**: Guizhou Province, Longli and Wengan counties, on leaves of *Hypericum patulum*, *Aralia chinensis* and *Acer palmatum*, June 2021, S.Y. Wang (HGUP 414, HGUP 412 and HGUP 405, living cultures GUCC 414.2, GUCC 414.21, GUCC 412.3, GUCC 405.6 and GUCC 405.16) (**new host and country record**).

Description: Asexual morph: Conidiomata pycnidial, separated, immersed or superficial, globose to depressed, initially appearing hyaline or light yellow becoming deep brown to black with age, up to 300 µm diam., 2–5 wall layers of dark brown textura angularis. *Conidiophores* reduced to conidiogenous cells. *Conidiogenous cells* central cushion of hyaline cells, densely aggregated, slightly thicker, subulate, simple, frequently branched above, tapering, hyaline, smooth, 12–22 × 3–4.5 µm ($\bar{x}$ = 17 × 3.5 µm; n = 15), surrounded by a gelatinous coating, apex with visible periclinal thickening. *Conidia* hyaline, asymmetrical, smooth-walled, cylindrical, slightly curved to naviculate, aseptate, rounded to acute apex, tapered to a subtruncate base, germ slits absent, 10–23 × 2.5–4.5 µm ($\bar{x}$ = 17 × 3.5 µm; n = 30). *Sexual morph:* Unknown.

Culture characteristics: Colonies covering 9 cm diam. Petri dish after 2 weeks at 25 °C and a 12 h light/dark regime; spreading with sparse aerial mycelium and uneven zonation. On PDA, surface with thin, white uneven zonated aerial mycelium, distinctly imbricated like a flower, producing a few pale yellow to dark brown to black conidial masses; reverse with white and pale brown, uneven zonated, imbricated aerial mycelium. On OA, surface with white or gray-white to pale yellow, fluffy, granular aerial mycelium, producing pale yellow to dark brown to black conidial masses from the centre; reverse white or beige to pale yellow.

Notes: Coniella quercicola was originally described as *Macroplodia quercicola*, from leaves of *Quercus robur* collected in the Netherlands. It was described as having pale brown, cylindrical conidia, 24 × 4 µm (Saccardo and Saccardo 1906). Our strains (GUCC 414.2, GUCC 414.21, GUCC 412.3, GUCC 405.6 and GUCC 405.16) are phylogenetically identical with the neotype culture (CBS 904.69) of *C. quercicola* isolated and designated by Alvarez et al. (2016) in ITS, LSU and *tef1* genes (Fig. 4). According to the results of DNA base comparison (Table 8), we note that base differences almost only occur in *tef1* region. is the present isolates of *C. quercicola* represent a new country record for China and new host records. Identificatiion of *C. quercicola* was based on its morphological characteristics, DNA phylogeny, DNA base differences and pairwise homoplasy index (PHI) test results.

Discussion

Families, genera, and species within *Diaporthales* are now characterized and separated based on a combination of morphology and molecular data (Voglmayr et al. 2012, 2017; Voglmayr and Jaklitsch 2014; Suetrong et al. 2015; Alvarez et al. 2016; Norphanphoun et al. 2016; Senanayake et al. 2017, 2018; Fan et al. 2018; Yang et al. 2018a; Guterres et al. 2019; Jiang and Tian 2019). The present study describes and

illustrates ten species (within five genera) of *Diaporthales* isolated from various host plants in Guizhou Province, China, including *Gnomoniopsis* mostly as host specific fungi (Sogonov et al. 2008; Walker et al. 2010; Jiang and Tian 2019; Yang et al. 2020). Based on their unique morphological characteristics, DNA phylogeny, DNA base differences and pairwise homoplasy index (PHI) test evaluation, we described one new genus, eight new species, and two new fungal records for China. Only asexual morphology was observed for all taxa described in this paper.

The molecular data provided evidence that our new genus is in *Foliocryphiaceae*, although in morphology it is similar to *Mastigosporella* in *Mastigosporellaceae*. In this molecular era, morphological conclusions are more and more being reduced to a subordinate, or even insignificant position. Thus, we accepted the phylogenetic conclusion to create *Pseudomastigosporella* as a monotypic genus. The traditional, visualized keys representing morphology are being replaced by novel, unseen phylograms. We need more strains of *Diaporthales*, in order to compare genome-wide information of members in this order because of high similarity in morphology but measurable difference in molecular data. Currently, there are too few data for comparison of fungi.

Except for *Diaporthe*, the five genera of *Diaporthales* presented in this paper did not produce conidial masses or spore-like masses on PDA medium. However, conidial masses were formed on OA medium within 1–2 weeks. Some *Diaporthe* species were more difficult to produce spores than those of the other four genera. Many authors have not only used traditional culture media (such as PDA, OA or MEA) to cultivate *Diaporthe* strains (Santos et al. 2011, 2017; Noriler et al. 2019; Hilário et al. 2020; Guo et al. 2020; Zapata et al. 2020), but have also used sterilized plant material such as pine needles, fennel twigs or alfalfa stems to induce sporulation and to obtain morphological data. Even with the addition of pine needles, it took longer (up to a month) for some *Diaporthe* species to produce spores than the other four genera of *Diaporthales* (personal experience). In our experience, OA medium was more conducive to sporulation of *Diaporthales* fungi than PDA medium. Its use is recommended for when describing morphological characteristics of *Diaporthales* species.

Conclusion

In this paper, we introduce ten species in five genera of *Diaporthales* from Guizhou Province, China, including one new genus, *Pseudomastigosporella*; eight new species, *Pseudomastigosporella guizhouensis*, *Chrysofolia coriariae*, *D. juglandigena*, *D. eucommiigena*, *D. dejiangensis*, *D. tongrensis*, *D. araliae-chinensis* and *D. hyperici*; and two new fungal records for China, *Gnomoniopsis rosae* and *Coniella quercicola*.

Abbreviations

ITS: Internal transcribed spacer; LSU: large ribosomal subunit (28S); *rpb2*: RNA polymerase II second largest subunit; *tef1*: translation elongation factor 1-alpha; *tub2*: beta-tubulin;
Ch.: *Chrysofolia*; *D.*: *Diaporthe*; *C*: *Coniella*; *G.*: *Gnomoniopsis*; *N.*: *Neocryphonectria*; *Ps.*: *Pseudocryphonectria*; PDA: potato dextrose agar; OA: oatmeal agar; MEA: malt extract agar; WA: water agar; NCBI: National Center for Biotechnology Information; ML: maximum likelihood; MP: maximum parsimony; BI: Bayesian inference;

GTR: general time reversible model; TL: Tree length; PT: Parsimonious tree; CI: Consistency indices; RI: Retention indices; RC: Rescaled consistency indices; HI: Homoplasy index; Model: the best nucleotide substitution model used for the different partitions; ASDSF: average standard deviation of split frequencies; MCMC: Markov chain Monte Carlo; PP: posterior probabilities; PHI: pin-pair homogeneity index test.

Declarations

Authors' contributions

Sampling, molecular biology analysis, fungal isolation, description and phylogenetic analysis, genome sequencing, assembly and gene annotation: Si-Yao Wang; writing original draft preparation: Si-Yao Wang; writing–review, editing and producing the final version: Si-Yao Wang, Yong Wang, Eric HC McKenzie, Alan JL Phillips and Yan Li. All authors read and approved the final manuscript.

Declarations

Ethics approval and consent to participate

Not applicable.

Adherence to national and international regulations

Not applicable.

Consent for publication

Not applicable.

Competing interests

The authors declare that they have no competing interests.

Author details

[1] Department of Plant Pathology, Agriculture College, Guizhou University, Guiyang, Guizhou Province, 550025, China. [2] Key Laboratory of Plant Resources Conservation and Germplasm Innovation in Mountainous Region (Ministry of Education), College of Life Sciences/Institute of Agro-Bioengineering, Guizhou University, Guiyang 550025, Guizhou Province, China. [3] Private Bag 92170, Auckland Mail Centre, Auckland 1142, New Zealand. [4] Universidade de Lisboa, Faculdade de Ciências, Biosystems and Integrative Sciences Institute (BioISI), Campo Grande, 1749-016 Lisbon, Portugal.

Availability of data and materials

All data generated or analysed during this study is included in this published article [and its supplementary information flies] and/or is available from the corresponding author upon reasonable request.

Acknowledgments

This research is supported by the following sources: The Open Project of Key Laboratory of Plant Resources Conservation and Germplasm Innovation in Mountainous Region (Ministry of Education) (MOELP-201801), and Postgraduate Education Innovation Program in Guizhou Province (YJSKYJJ [2021] 058). Alan JL Phillips acknowledges the support from UIDB/04046/2020 and UIDP/04046/2020 Centre grants from FCT, Portugal (to BioISI).

References

Alexopoulus CJ, Mims CW (1978) Introductory mycology, 3rd edn. Wiley, New York.

Alvarez LV, Groenewald JZ, Crous PW (2016) Revising the Schizoparmaceae: *Coniella* and its synonyms *Pilidiella* and *Schizoparme*. Stud Mycol 85:1–34. https://doi.org/10.1016/j.simyco.2016.09.001

Barr ME (1978) The Diaporthales in North America: with emphasis on *Gnomonia* and its segregates. Mycol Mem 7:1–232

Bruen TC, Philippe H, Bryant D (2006) A simple and robust statistical test for detecting the presence of recombination. Genetics 172:2665–2681. https://doi.org/10.1534/genetics.105.048975

Carbone I, Kohn LM (1999) A method for designing primer sets for speciation studies in filamentous ascomycetes. Mycologia 91:553–556. https://doi.org/10.1080/00275514.1999.12061051

Castlebury LA, Rossman AY, Jaklitsch WJ, Vasilyeva LN (2002) A preliminary overview of the Diaporthales based on large subunit nuclear ribosomal DNA sequences. Mycologia 94:1017–1031. https://doi.org/10.1080/15572536.2003.11833157

Chang CQ, Xi PG, Xiang MM et al (2005) New species of *Phomopsis* on woody plants in Hunan province. Mycosystema 24:145–154. https://doi.org/10.3969/j.issn.1672-6472.2005.01.002

Cheewangkoon R, Groenewald JZ, Summerell BA et al (2009) Myrtaceae, a cache of fungal biodiversity. Persoonia 23:55–85. https://doi.org/10.3767/003158509X474752

Chomnunti P, Hongsanan S, Aguirre-Hudson B et al (2014) The sooty moulds. Fungal Divers 66:1–36. https://doi.org/10.1007/s13225-014-0278-5

Crous PW, Gams W, Stalpers JA, Robert V, Stegehuis G (2004) MycoBank: an online initiative to launch mycology into the 21st century. Studies in Mycology 50:19–22.

Crous PW, Luangsa-Ard JJ, Wingfield MJ et al (2018) Fungal planet description sheets 785–867. Persoonia 41:238–417. https://doi.org/10.3767/persoonia.2018.41.12

Crous PW, Summerell BA, Shivas RG et al (2012) Fungal planet description sheets: 107–127. Persoonia 28:138–182. https://doi.org/10.3767/003158512X652633

Crous PW, Wingfield MJ, Guarro J et al (2015) Fungal planet description sheets: 320–370. Persoonia 34:167–266. https://doi.org/10.3767/003158515X688433

Crous PW, Wingfield MJ, Schumacher RK et al (2014) Fungal Planet Description Sheets: 281–319. Persoonia 33:212–289. https://doi.org/10.3767/003158514X685680

Fan XL, Bezerra JD, Tian CM, Crous PW (2018) Families and genera of diaporthalean fungi associated with canker and dieback of tree hosts. Persoonia 40:119–134. https://doi.org/10.3767/persoonia.2018.40.05

Gao YH, Su YY, Sun W, Cai L (2014) Three new species of *Phomopsis* in Gutianshan nature reserve in China. Mycol Progress 13:111–121. https://doi.org/10.1007/s11557-013-0898-2

Glass NL, Donaldson G (1995) Development of primer sets designed for use with PCR to amplify conserved genes from filamentous ascomycetes. Applied and Environmental Microbiology 61:1323–1330. https://doi.org/10.1128/aem.61.4.1323-1330.1995

Gomes RR, Glienke C, Videira SIR et al (2013) *Diaporthe*: a genus of endophytic, saprobic and plant pathogenic fungi. Persoonia 31:1–41. https://doi.org/10.3767/003158513X666844

Guarnaccia V, Groenewald JZ, Woodhall J et al (2018) *Diaporthe* diversity and pathogenicity revealed from a broad survey of grapevine diseases in Europe. Persoonia 40:135–153. https://doi.org/10.3767/persoonia.2018.40.06

Guo YS, Crous PW, Bai Q et al (2020) High diversity of *Diaporthe* species associated with pear shoot canker in China. Persoonia 45:132–162. https://doi.org/10.3767/persoonia.2020.45.05

Guterres DC, Galvão-Elias S, Santos MDDM et al (2019) Phylogenetic relationships of *Phaeochorella parinarii* and recognition of a new family, Phaeochorellaceae (Diaporthales). Mycologia 111:660–675. https://doi.org/10.1080/00275514.2019.1603025

Hall TA (1999) BioEdit: a user-friendly biological sequence alignment editor and analysis program for Windows 95/98/NT. Nucleic Acids Symposium Series 41:95–98. https://doi.org/10.1021/bk-1999-0734.ch008

Hawksworth DL, Kirk PM, Sutton BC, Pegler DN (1995) Ainsworth & Bisby's dictionary of the fungi. 8th ed. reprinted. Oxford, U.K.: CAB International.

Hespanhol L, Vallio CS, Costa LM, Saragiotto BT (2019) Understanding and interpreting confidence and credible intervals around effect estimates. Brazilian Journal of Physical Therapy 23:290–301. https://doi.org/10.1016/j.bjpt.2018.12.006

Hilário S, Amaral I, Gonçalves MFM et al (2020) *Diaporthe* species associated with twig blight and dieback of *Vaccinium corymbosum* in Portugal, with description of four new species. Mycologia 112:293–308. https://doi.org/10.1080/00275514.2019.1698926

Hillis DM, Bull JJ (1993) An empirical test of bootstrapping as a method for assessing confidence in phylogenetic analysis. Systematic Biology 42:182–192. https://doi.org/10.1093/ sysbio/42.2.182

Höhnel FV (1918) Dritte vorlaufige Mitteilung mycologischer Ergebnisse (Nr. 201–304). Berichte der Deutschen Botanischen Gesellschaft 36:309–317

Huson DH (1998) SplitsTree: analyzing and visualizing evolutionary data. Bioinformatics 14:68–73. https://doi.org/10.1093/bioinformatics/14.1.68

Huson DH, Bryant D (2006) Application of phylogenetic networks in evolutionary studies. Molecular Biology and Evolution 23:254–267. https://doi.org/10.1093/molbev/msj030

Hyde KD, Dong Y, Phookamsak RT et al (2020) Fungal diversity notes 1151–1276: taxonomic and phylogenetic contributions on genera and species of fungal taxa. Fungal Divers 100:5–277. https://doi.org/10.1007/s13225-020-00439-5

Jiang N, Fan XL, Tian CM, Crous PW (2020) Reevaluating Cryphonectriaceae and allied families in Diaporthales. Mycologia 112:267–292. https://doi.org/10.1080/00275514.2019.1698925

Jiang N, Tian CM (2019) An emerging pathogen from rotted chestnut in China: *Gnomoniopsis daii* sp. nov. Forests 10:1016. https://doi.org/10.3390/f10111016

Katoh K, Standley DM (2016) A simple method to control over-alignment in the MAFFT multiple sequence alignment program. Bioinformatics 32:1933–1942. https://doi.org/10.1093/bioinformatics/btw108

Larsson A (2014) AliView: a fast and lightweight alignment viewer and editor for large datasets. Bioinformatics 22:3276–3278. https://doi.org/10.1093/bioinformatics/btu531

Liu Y, Whelen S, Hall BD (1999) Phylogenetic relationships among ascomycetes: evidence from an RNA polymerase II subunit. Molecular Biology and Evolution 16:1799–1808. https://doi.org/10.1093/oxfordjournals.molbev.a026092

Maharachchikumbura SSN, Hyde KD, Jones EBG et al (2015) Towards a natural classification and backbone tree for Sordariomycetes. Fungal Divers 72:199–301. https://doi.org/10.1007/s13225-015-0331-z

Maharachchikumbura SSN, Hyde KD, Jones EBG et al (2016) Families of Sordariomycetes. Fungal Divers 79:1–317. https://doi.org/10.1007/s13225-016-0369-6

Mejía LC, Castlebury LA, Rossman AY et al (2011a) A systematic account of the genus *Plagiostoma* (Gnomoniaceae, Diaporthales) based on morphology, host-associations, and a four-gene phylogeny. Stud Mycol 68:211–235. https://doi.org/10.3114/sim.2011.68.10

Mejía LC, Rossman AY, Castlebury LA, White JF (2011b) New species, phylogeny, host-associations and geographic distribution of genus *Cryptosporella* (Gnomoniaceae, Diaporthales). Mycologia 103:379–399. https://doi.org/10.3852/10-134

Mejía LC, Rossman AY, Castlebury LA et al (2012) *Occultocarpon*, a new monotypic genus of Gnomoniaceae on *Alnus nepalensis* from China. Fungal Divers 52:99–105. https://doi.org/10.1007/s13225-011-0108-y

Miller MA, Pfeiffer W, Schwartz T (2010) Creating the CIPRES Science Gateway for inference of large phylogenetic trees. In: Proceeding of the 2010 gateway computing environments workshop (GCE), New Orleans, Louisiana 1–8

Monod M (1983) Taxonomic monograph of the Gnomoniaceae (Ascomycetes of the ordre Diaporthales). I. Beihefte zur Sydowia 9:1–315

Noriler SA , Savi DC, Ponomareva LV et al (2019) Vochysiamides A and B: Two new bioactive carboxamides produced by the new species *Diaporthe vochysiae*. Fitoterapia 138:104273. https://doi.org/10.1016/j.fitote.2019.104273

Norphanphoun C, Hongsanan S, Doilom M et al (2016) *Lamproconiaceae* fam. nov. to accommodate *Lamproconium desmazieri.* Phytotaxa 270:89–102. https://doi.org/10.11646/phytotaxa.270.4

Nylander JA, Wilgenbusch JC, Warren DL, Swofford DL (2008) AWTY: A system for graphical exploration of MCMC convergence in Bayesian phylogenetics. Bioinformatics 24:581–583. https://doi.org/10.1093/bioinformatics/btm388

Petrak F, Sydow H (1927) Die Gattungen der Pyrenomyzeten, Sphaeropsideen und Melanconieen. I. Der phaeosporen Sphaeropsideen und die Gattung *Macrophoma*. Feddes Repertorium Speciarum Novarum Regni Vegetabilum Beihefte 42:1–551

Quaedvlieg W, Binder M, Groenewald JZ et al (2014) Introducing the consolidated species concept to resolve species in the Teratosphaeriaceae. Persoonia 33:1–40.

https://doi.org/10.3767/003158514X681981

Rambaut A (2016) FigTree-version 1.4.3, a graphical viewer of phylogenetic trees. Available at: http://tree.bio.ed.ac.uk/software/figtree (Accessed October 5, 2016)

Rannala B, Yang ZH (1996) Probability distribution of molecular evolutionary trees: A new method of phylogenetic inference. Journal of Molecular Evolution 43:304–311. https://doi.org/10.1007/BF02338839

Raudabaugh DB, Iturriaga T, Carver A et al (2018) *Coniella lustricola*, a new species from submerged detritus. Mycol Progress 17:191–203. https://doi.org/10.1007/s11557-017-1337-6

Rehner SA, Samuels GJ (1995) Molecular systematics of the Hypocreales: a teleomorph gene phylogeny and the status of their anamorphs. Canadian Journal of Botany 73:816–823

Ronquist F, Teslenko M, Mark VD et al (2012) MrBayes 3.2: efficient Bayesian phylogenetic inference and model choice across a large model space. Systematic Biology 61:539–542. https://doi.org/10.1093/sysbio/sys029

Rossman AY, Farr DF, Castlebury LA (2007) A review of the phylogeny and biology of the Diaporthales. Mycoscience 48:135–144. https://doi.org/10.1007/S10267-007-0347-7

Saccardo PA, Saccardo D (1906) Supplementum universale. Pars VII. Discomycetae-Deuteromycatae. Sylloge Fungorum 18:1–838

Santos JM, Vrandecic K, Cosic J et al (2011) Resolving the *Diaporthe* species occurring on soybean in Croatia. Persoonia 27:9–19. https://doi.org/10.3767/003158511X603719

Santos L, Phillips AJL, Crous PW, Alves A (2017) *Diaporthe* species on Rosaceae with descriptions of *D. pyracanthae* sp. nov. and *D. malorum* sp. nov. Mycosphere 8:485–511. https://doi.org/10.5943/mycosphere/8/5/1

Senanayake IC, Crous PW, Groenewald JZ et al (2017) Families of Diaporthales based on morphological and phylogenetic evidence. Stud Mycol 86:217–296. https://doi.org/10.1016/j.simyco.2017.07.003

Senanayake IC, Jeewon R, Chomnunti P et al (2018) Taxonomic circumscription of Diaporthales based on multigene phylogeny and morphology. Fungal Divers 93:241–443. https://doi.org/10.1007/s13225-018-0410-z

Sogonov MV, Castlebury LA, Rossman AY et al (2008) Leaf-inhabiting genera of the Gnomoniaceae, Diaporthales. Stud Mycol 62:1–77. https://doi.org/10.3114/sim.2008.62.01

Stamatakis A (2006) RAxML-VI-HPC: maximum likelihood-based phylogenetic analyses with thousands of taxa and mixed models. Bioinformatics 22:2688–2690. https://doi.org/10.1093/bioinformatics/btl446

Suetrong S, Klaysuban A, Sakayaroj J et al (2015) Tiarisporellaceae, a new family in the order Diaporthales (Sordariomycetes, Ascomycota). Cryptogamie Mycologie 36:319–330. https://doi.org/10.7872/crym/v36.iss3.2015.319

Suwannarach N, Kumla J, Sri-Ngernyuang K, Lumyong S (2016) A new endophytic fungus, *Chrysofolia barringtoniae* sp. nov. from Thailand. Mycoscience 57:361–365. https://doi.org/10.1016/j.myc.2016.06.003

Taylor JW, Jacobson DJ, Kroken S et al (2000) Phylogenetic species recognition and species concepts in fungi. Fungal Genetics and Biology 31:21–32. https://doi.org/10.1006/fgbi.2000.1228

Tennakoon DS, Kuo CH, Maharachchikumbura SSN et al (2021) Taxonomic and phylogenetic contributions to *Celtis formosana*, *Ficus ampelas*, *F. septica*, *Macaranga tanarius* and *Morus australis* leaf litter inhabiting microfungi. Fungal Divers 108:1–215. https://doi.org/10.1007/s13225-021-00474-w

Udayanga SD, Liu XZ, Crous PW et al (2012) A multi-locus phylogenetic evaluation of *Diaporthe* (*Phomopsis*). Fungal Divers 56:157–171. https://doi.org/10.1007/s13225-012-0190-9

Udayanga SD, Liu XZ, McKenzie EHC et al (2011) The genus *Phomopsis*: biology, applications, species concepts and names of common phytopathogens. Fungal Divers 50:189. https://doi.org/10.1007/s13225-011-0126-9

Vaidya G, Lohman DJ, Meier R (2011) SequenceMatrix: concatenation software for the fast assembly of multi-gene datasets with character set and codon information. Cladistics 27:171–180. https://doi.org/10.1111/j.1096-0031.2010.00329.x

Vasilyeva LN, Rossman AY, Farr DF (2007) New species of the Diaporthales from eastern Asia and eastern North America. Mycologia 99:916–923. https://doi.org/10.1080/15572536.2007.11832523

Vilgalys R, Hester M (1990) Rapid genetic identification and mapping of enzymatically amplified ribosomal DNA from several *Cryptococcus* species. Journal of Bacteriology 172:4238–4246. https://doi.org/10.1128/jb.172.8.4238-4246.1990

Voglmayr H, Castlebury LA, Jaklitsch WM (2017) *Juglanconis* gen. nov. on Juglandaceae, and the new family Juglanconidaceae (Diaporthales). Persoonia 38:136–155. https://doi.org/10.3767/003158517X694768

Voglmayr H, Jaklitsch WM (2014) Stilbosporaceae resurrected: generic reclassification and speciation. Persoonia 33:61–82. https://doi.org/10.3767/003158514X684212

Voglmayr H, Rossman AY, Castlebury LA, Jaklitsch WM (2012) Multigene phylogeny and taxonomy of the genus *Melanconiella* (Diaporthales). Fungal Divers 57:1–44. https://doi.org/10.1007/s13225-012-0175-8

Walker DM, Castlebury LA, Rossman AY et al (2010) Systematics of genus *Gnomoniopsis* (Gnomoniaceae, Diaporthales) based on a three gene phylogeny, host associations and morphology. Mycologia 102:1479–1496. https://doi.org/10.3852/10-002

Walker DM, Castlebury LA, Rossman AY et al (2012) Phylogeny and taxonomy of *Ophiognomonia* (Gnomoniaceae, Diaporthales), including twenty-five new species in this highly diverse genus. Fungal Divers 57:85–147. https://doi.org/10.1007/s13225-012-0200-y

White TJ, Bruns T, Lee S, Taylor JW (1990) Amplification and direct sequencing of fungal ribosomal RNA genes for phylogenetics. In: Innis, M., Gelfand, D, Shinsky, J. & White, T. (Eds) PCR protocols: a guide to methods and applications 18:315–322. https://doi. org/10.1016/B978-0-12-372180-8.50042-1

Yang Q, Fan XL, Du Z, Tian CM (2018a) Diaporthosporellaceae, a novel family of Diaporthales (Sordariomycetes, Ascomycota). Mycoscience 59:229–235. https://doi.org/10.1016/j.myc.2017.11.005

Yang Q, Fan XL, Guarnaccia V, Tian CM (2018b) High diversity of *Diaporthe* species associated with dieback diseases in China, with twelve new species described. MycoKeys 39:97–149. https://doi.org/10.3897/mycokeys.39.26914

Yang Q, Jiang N, Tian CM (2020) Three new *Diaporthe* species from Shaanxi Province, China. MycoKeys 67:1–18. https://doi.org/10.3897/mycokeys.67.49483

Zapata M, Palma MA, Aninat MJ, Piontelli E (2020) Polyphasic studies of new species of *Diaporthe* from native forest in Chile, with descriptions of *Diaporthe araucanorum* sp. nov., *Diaporthe foikelawen* sp. nov. and

Diaporthe patagonica sp. nov. International Journal of Systematic and Evolutionary Microbiology 70:3379–3390. https://doi.org/10.1099/ ijsem.0.004183

Zhang ZF, Liu F, Zhou X et al (2017) Culturable mycobiota from Karst caves in China, with descriptions of 20 new species. Persoonia 39:1–31. https://doi.org/10.3767/persoonia.2017.39.01

Tables

Table 2. Strains and their GenBank accession numbers used in the molecular phylogenetic analyses of *Foliocryphiaceae*. (^{T}) = ex-type strain.

Species	Strain number	GenBank Accession number				
		ITS	LSU	*rpb2*	*tef1*	*tub2*
Amphilogia gyrosa	CBS 112922^T	AF452111	AY194107	MN271782	MN271818	AF525714
Aurantioporthe corni	CBS 245.90	MN172403	MN172371	MN271784	MN271822	–
Aurantiosacculus acutatus	CBS 132181^T	JQ685514	JQ685520	–	MN271823	–
Aurantiosacculus castaneae	CFCC 52456^T	MH514025	MH514015	MN271786	–	MH539688
Aurantiosacculus eucalyptorum	CPC 13229^T	JQ685515	JQ685521	MN271785	MN271824	–
Aurapex penicillata	CMW 10030^T	AY214311	AY194103	MN271787	–	AY214239
Aurifilum marmelostoma	CBS 124928^T	MH863426	MH874934	MN271788	MN271827	MN987000
Aurifilum terminali	CSF10762	MN199838	MN258786	–	MN258781	MN258771
Celoporthe dispersa	CBS 118782^T	DQ267130	HQ730853	–	HQ730840	AY214280
Celoporthe eucalypti	CMW 26908^T	HQ730837	HQ730863	MN271790	HQ730850	MN263386
Chrysofolia barringtoniae	TBRC 5647	KU948046	KU948045	–	–	–
Chrysofolia colombiana	CPC 24986^T	KR476738	KR476771	–	MN271829	–
Chrysomorbus lagerstroemiae	CBS 142594^T	KY929338	KY929328	–	MN271830	KY929348
Chrysoporthe hodgesiana	CBS 115854^T	AY692322	MN172380	MN271793	MN271836	–
Chrysoporthe syzygiicola	CBS 124488^T	FJ655005	MN172383	–	MN271839	FJ805236
Corticimorbus sinomyrti	CBS 140205^T	KT167169	KT167179	MN271794	MN271841	KT167183
Cryphonectria macrospora	CBS 109764	EU199182	AF408340	EU220029	KC465405	AH014594
Cryphonectria parasitica	ATCC 38755	MH843497	MH514021	DQ862017	MN271848	MW086477
Cryptometrion aestuescens	CBS 124014^T	MH863335	MH874864	MN271798	MN271851	GQ369456
Diversimorbus metrosideri	CBS 132866^T	JQ862871	JQ862828	–	MN271857	JQ862953
Dwiroopa lythri	CBS 109755^T	MN172410	MN172389	MN271801	MN271859	–
Dwiroopa punicae	CBS 143163^T	MK510676	MK510686	MK510692	MH020056	MK510714
Endothia chinensis	CFCC 52144^T	MH514027	MH514017	–	MN271860	MH539690
Foliocryphia eucalypti	CBS 124779^T	GQ303276	GQ303307	MN271802	MN271861	JQ706128
Foliocryphia eucalyptorum	CBS 142536^T	KY979772	KY979827	MN271803	MN271862	KY979936
Holocryphia capensis	CBS 132870^T	JQ862854	JQ862811	–	MN271883	JQ862948
Holocryphia eucalypti	CBS 115842^T	MN172411	MN172391	MN271804	MN271882	JQ862772
Immersiporthe knoxdaviesiana	CBS 132862^T	JQ862765	JQ862755	MN271805	MN271886	JQ862785
Latruncellus aurorae	CBS 125526^T	GU726947	HQ730872	–	MN271888	GU726959
Luteocirrhus shearii	CBS 130776^T	KC197021	KC197019	MN271807	MN271890	KC197006
Microthia havanensis	CBS 115855	DQ368735	MN172393	MN271811	–	–
Myrtonectria myrtacearum	CMW 46433^T	MG585736	MG585750	–	–	MG585734
Neocryphonectria carpini	CFCC 53027^T	MN172413	MN172396	–	–	–
Neocryphonectria chinensis	CFCC 53025^T	MN172414	MN172397	MN271812	MN271893	–
Neocryphonectria chinensis	CFCC 53029	MN172415	MN172398	MN271813	MN271894	–
Rostraureum tropicale	CBS 115725^T	AY167435	MN172399	MN271814	MN271895	AY167431
Ursicollum fallax	CBS 118663^T	DQ368755	EF392860	MN271816	MN271897	AH015658

Table 3. Strains and their GenBank accession numbers used in the molecular phylogenetic analyses of *Diaporthe*. (^{T}) = ex–type strain.

Species	Strain number	GenBank Accession number		
		ITS	*tef1*	*tub2*
Diaporthe australafricana	CBS 111886^{T}	KC343038	KC343764	KC344006
D. australiana	BRIP 66145^{T}	MN708222	MN696522	MN696530
D. beckhausii	CBS 138.27	KC343041	KC343767	KC344009
D. benedicti	CFCC 50062^{T}	KP208847	KP208853	KP208855
D. bohemiae	CBS 143347^{T}	MG281015	MG281536	MG281188
D. brasiliensis	CBS 133183^{T}	KC343042	KC343768	KC344010
D. caatingaensis	CBS 141542^{T}	KY085927	KY115603	KY115600
D. carpini	CBS 114437	KC343044	KC343770	KC344012
D. caryae	CFCC 52563^{T}	MH121498	MH121540	MH121580
D. caryae	PSCG520	MK626952	MK654895	MK691315
D. cassines	CPC 21916^{T}	KF777155	KF777244	–
D. caulivora	CBS 127268^{T}	KC343045	KC343771	KC344013
D. caulivora	Dip1	HM347703	HM347687	–
D. caulivora	Dpc11	HM347704	HM347688	–
D. chimonanthi	HGUP191001	MZ724752	–	MZ724033
D. chimonanthi	HGUP192087	MZ724753	–	MZ724034
D. cotoneastri	CBS 439.82^{T}	MH861511	GQ250341	JX275437
D. cynaroidis	CBS 122676^{T}	KC343058	KC343784	KC344026
D. ellipicola	CGMCC 3.17084^{T}	KF576270	KF576245	KF576294
D. ellipicola	CGMCC 3.17085	KF576271	KF576246	KF576295
D. eres	CBS 138594^{T}	KJ210529	KJ210550	KJ420799
D. eres	CAA801	KY435644	KY435631	KY435672
D. fibrosa	CBS 109751	KC343099	KC343825	KC344067
D. fusicola	CGMCC 3.17087^{T}	KF576281	KF576256	KF576305
D. fusiformis	JZB320154	MW010216	–	MW056012
D. fusiformis	JZB320155	MW010217	–	MW056013
D. hongkongensis	CBS 115448^{T}	KC343119	KC343845	KC344087
D. impulsa	CBS 114434	KC343121	KC343847	KC344089
D. italiana	MFLUCC 18-0090^{T}	MH846237	MH853686	MH853688
D. lithocarpus	CGMCC 3.15175^{T}	KC153104	KC153095	KF576311
D. lithocarpus	CGMCC 3.15177	KC153100	KC153091	–
D. longicolla	ATCC 60325^{T}	KJ590728	KJ590767	KJ610883
D. longicolla	1-2/4-3	HM347711	HM347682	–
D. malorum	CAA734^{T}	KY435638	KY435627	KY435668
D. malorum	CAA740	KY435642	KY435629	KY435670
D. malorum	CAA752	KY435643	KY435630	KY435671
D. mediterranea	DAL-176	MT007496	MT006996	MT006693
D. nobilis	CBS 124030	KC343149	KC343875	KC344117
D. nobilis	JZB320158	MG557846	MG557848	MG557847
D. nothofagi	BRIP 54801^{T}	JX862530	JX862536	KF170922
D. ocoteae	CBS 141330^{T}	KX228293	–	KX228388
D. ovoicicola	CGMCC 3.17092^{T}	KF576264	KF576239	KF576288
D. paranensis	CBS 133184^{T}	KC343171	KC343897	KC344139
D. passiflorae	CBS 132527^{T}	JX069860	KY435633	KY435674
D. phaseolorum	Ar2	HM347705	HM347679	–
D. phaseolorum	CBS 127266	HM347707	HM347672	HQ333513
D. phragmitis	CBS 138897^{T}	KP004445	–	KP004507
D. rudis	CBS 109292^{T}	KC343234	KC343960	KC344202
D. salicicola	BRIP 54825^{T}	JX862531	JX862537	KF170923
D. subcylindrospora	KUMCC 17-0151	MG746629	MG746630	MG746631
D. tectonigena	MFLUCC 12-0767^{T}	KU712429	KU749371	KU743976
D. ueckerae	FAU656^{T}	KJ590726	KJ590747	KJ610881
D. xishuangbanica	CGMCC 3.18282^{T}	KX986783	KX999175	KX999216
Diaporthella corylina	CBS 121124^{T}	KC343004	KC343730	KC343972

Table 4. Strains and their GenBank accession numbers used in the molecular phylogenetic analyses of *Gnomoniopsis*. (^{T}) = ex–type strain.

Species	Strain number	GenBank Accession number				
		ITS	LSU	*rpb2*	*tef1*	*tub2*
Gnomoniopsis alderdunense	CBS 125681	GU320827	MH875098	–	GU320802	GU320789
G. alderdunensis	CBS 125680^T	MH863625	MH875097	–	GU320801	GU320787
G. angolensis	CBS 145057^T	MK047428	MK047479	MK047539	–	–
G. castaneae	GCAS5	MH107830	MZ682110	–	MH213486	MH213481
G. castanopsidis	CFCC 54437^T	MZ902909	–	–	MZ936385	
G. chamaemori	CBS 803.79	EU254808	EU255107	–	GU320809	EU219155
G. chinensis	CFCC 52286^T	MG866032	–	–	MH545370	MH545366
G. clavulata	AR 4313	EU254818	–	EU219251	EU221934	EU219211
G. comari	CBS 806.79^T	EU254821	EU255114	EU219286	GU320810	EU219156
G. daii	CFCC 55517	MZ902911	–	–	MZ936387	MZ936403
G. fagacearum	CFCC 54316^T	MZ902916	–	–	MZ936392	MZ936408
G. fructicola (=*G. fragariae*)	CBS 125671	MH863616	MH875088	–	GU320793	GU320776
G. guangdongensis	CFCC 54443^T	MZ902918	–	–	MZ936394	MZ936410
G. hainanensis	CFCC 54376^T	MZ902921	–	–	MZ936397	MZ936413
G. idaeicola	CBS 125674^T	MH863619	MH875091	–	GU320796	GU320780
G. macounii	CBS 121468^T	MH863110	MH874666	–	GU320804	–
G. occulta	CBS 125678	MH863623	MH875095	–	GU320800	GU320786
G. paraclavulata	CBS 123202^T	GU320830	–	–	GU320815	GU320775
G. racemula	AR 3892	EU254841	EU255122	EU219241	EU221889	EU219125
G. rosae	CBS 145085	MK047451	MK047501	MK047547	–	–
G. rossmaniae	CFCC 54307^T	MZ902923	–	–	MZ936399	MZ936415
G. sanguisorbae	CBS 858.79	GU320818	KY496735	–	GU320805	GU320790
G. silvicola	CFCC 54418^T	MZ902926	–	–	MZ936402	MZ936418
G. smithogilvyi	CBS 130190^T	MH865607	MH877031	JQ910648	JQ910645	JQ910639
G. tormentillae	CBS 904.79	EU254856	EU255133	–	GU320795	EU219165
G. xunwuensis	CFCC 53115T	MK432667	MK429910	–	MK578141	MK578067
Sirococcus tsugae	CBS 119626	EF512472	–	–	EF512534	EU219140

Table 5. Strains and their GenBank accession numbers used in the molecular phylogenetic analyses of *Coniella*. (^{T}) = ex–type strain.

Species	Strain number	GenBank Accession number		
		ITS	LSU	*tef1*
Coniella africana	CBS 114133^{T}	AY339344	AY339293	KX833600
C. diplodiella	CBS 111858^{T}	MH862886	KX833335	KX833603
C. diplodiella	CBS 165.84	KX833529	KX833354	KX833622
C. erumpens	CBS 523.78^{T}	KX833535	KX833361	KX833630
C. eucalyptorum	CBS 112640^{T}	AY339338	AY339290	KX833637
C. fusiformis	CBS 141596^{T}	KX833576	KX833397	KX833674
C. granati	CBS 130974	JN815312	KX833398	KX833675
C. granati	CBS 252.38	KX833581	AY339291	KX833681
C. hibisci	CBS 109757^{T}	KX833589	AF408337	KX833689
C. javanica	CBS 455.68^{T}	KX833583	KX833403	KX833683
C. koreana	CBS 143.97^{T}	KX833584	AF408378	KX833684
C. koreana	CFCC 52986	MK432612	MK429882	MK578112
C. lanneae	CBS 141597^{T}	KX833585	KX833404	KX833685
C. limoniformis	CBS 111021^{T}	KX833586	KX833405	KX833686
C. macrospora	CBS 524.73^{T}	KX833587	AY339292	KX833687
C. macrospora	STE-U 3935	AY339343	–	AY339363
C. malaysiana	CBS 141598^{T}	KX833588	KX833406	KX833688
C. nicotianae	CBS 875.72^{T}	KX833590	KX833407	KX833690
C. pseudostraminea	CBS 112624^{T}	KX833593	KX833412	KX833696
C. quercicola	CBS 904.69^{T}	KX833595	KX833414	KX833698
C. quercicola	CBS 283.76	KX833594	KX833413	KX833697
C. quercicola	CPC 12133	KX833596	–	KX833699
C. straminea	CBS 149.22	AY339348	AY339296	KX833704
C. tibouchinae	CBS 131594^{T}	JQ281774	KX833418	JQ281778
C. tibouchinae	CBS 131595	JQ281775	KX833419	JQ281779
C. fragariae	CBS 172.49^{T}	AY339317	AY339282	KX833663
C. nigra	CBS 165.60^{T}	AY339319	KX833408	KX833691

Table 6. Species, strain information and GenBank accession numbers for sequences obtained in this study. (^{T}) = ex–type strain.

Species	Strain number	Host	GenBank Accession number				
			ITS	LSU	*rpb2*	*tef1*	*tub2*
Chrysofolia coriariae sp. nov.	GUCC 416.4^{T}	*Coriaria nepalensis*	OP581211	OP581237	n/a	OP688516	OP688542
Chrysofolia coriariae sp. nov.	GUCC 416.14	*Coriaria nepalensis*	OP581212	OP581238	n/a	OP688517	OP688543
Coniella quercicola	GUCC 414.2	*Hypericum patulum*	OP581213	OP581239	n/a	OP688518	OP688544
Coniella quercicola	GUCC 414.21	*Hypericum patulum*	OP581214	OP581240	n/a	OP688519	OP688545
Coniella quercicola	GUCC 412.3	*Aralia chinensis*	OP581215	OP581241	n/a	OP688520	n/a
Coniella quercicola	GUCC 405.6	*Acer palmatum*	OP581216	OP581242	n/a	OP688521	OP688546
Coniella quercicola	GUCC 405.16	*Acer palmatum*	OP581217	OP581243	n/a	OP688522	OP688547
Diaporthe araliae-chinensis sp. nov.	GUCC 412.7^{T}	*Aralia chinensis*	OP581218	n/a	n/a	OP688523	OP688548
Diaporthe araliae-chinensis sp. nov.	GUCC 412.71	*Aralia chinensis*	OP581219	n/a	n/a	OP688524	OP688549
Diaporthe araliae-chinensis sp. nov.	GUCC 412.17	*Aralia chinensis*	OP581220	n/a	n/a	OP688525	OP688550
Diaporthe dejiangensis sp. nov.	GUCC 421.2^{T}	*Juglans regia*	OP581221	n/a	n/a	OP688526	OP688551
Diaporthe dejiangensis sp. nov.	GUCC 421.21	*Juglans regia*	OP581222	n/a	n/a	OP688527	OP688552
Diaporthe eucommiigena sp. nov.	GUCC 420.9^{T}	*Eucommia ulmoides*	OP581223	n/a	n/a	OP688528	OP688553
Diaporthe eucommiigena sp. nov.	GUCC 420.19	*Eucommia ulmoides*	OP581224	n/a	n/a	OP688529	OP688554
Diaporthe tongrensis sp. nov.	GUCC 421.10^{T}	*Juglans regia*	OP581225	n/a	n/a	OP688530	OP688555
Diaporthe tongrensis sp. nov.	GUCC 421.101	*Juglans regia*	OP581226	n/a	n/a	OP688531	OP688556
Diaporthe hyperici sp. nov.	GUCC 414.4^{T}	*Hypericum patulum*	OP581227	n/a	n/a	OP688532	OP688557
Diaporthe hyperici sp. nov.	GUCC 414.14	*Hypericum patulum*	OP581228	n/a	n/a	OP688533	OP688558
Diaporthe juglandigena sp. nov.	GUCC 422.16^{T}	*Juglans regia*	OP581229	n/a	n/a	OP688534	OP688559
Diaporthe juglandigena sp. nov.	GUCC 422.161	*Juglans regia*	OP581230	n/a	n/a	OP688535	OP688560
Gnomoniopsis rosae	GUCC 408.7	*Rosa sp.*	OP581231	OP581244	OP688512	OP688536	OP688561
Gnomoniopsis rosae	GUCC 408.17	*Rosa sp.*	OP581232	OP581245	OP688513	OP688537	OP688562
Pseudomastigosporella guizhouensis sp. nov.	GUCC 406.6^{T}	*Hypericum patulum*	OP581233	OP581246	OP688514	OP688538	OP688563
Pseudomastigosporella guizhouensis sp. nov.	GUCC 405.3	*Acer palmatum*	OP581234	OP581247	OP688515	OP688539	OP688564
Pseudomastigosporella guizhouensis sp. nov.	GUCC 405.4	*Acer palmatum*	OP581235	OP581248	n/a	OP688540	OP688565
Pseudomastigosporella guizhouensis sp. nov.	GUCC 405.8	*Acer palmatum*	OP581236	OP581249	n/a	OP688541	OP688566

Table 8. DNA base differences between our strains and related taxa in the five-locus regions. Asterisks (*) denote our material. (^{T}) = ex–type strain.

Species	Strain number	Gene region and alignment positions				
		ITS (1–769 characters)	LSU (770–1617 characters)	*rpb2* (1618–2442 characters)	*tef1* (2443–2952 characters)	*tub2* (2953–3596 characters)
		(with gap: 151 characters)	(with gap: 41 characters)	(no data)	(no data)	(no data)
Chrysofolia barringtoniae	TBRC 5647	–	–	n/a	n/a	n/a
Chrysofolia coriariae sp. nov.*	GUCC 416.4^{T}	31	4	n/a	n/a	n/a
Chrysofolia coriariae sp. nov.*	GUCC 416.14	31	4	n/a	n/a	n/a
		(with gap: 158 characters)	(with gap: 41 characters)	(no data)	(with gap:156 characters)	(no data)
Chrysofolia colombiana	CPC 24986	–	–	n/a	–	n/a
Chrysofolia coriariae sp. nov.*	GUCC 416.4^{T}	7	2	n/a	149	n/a
Chrysofolia coriariae sp. nov.*	GUCC 416.14	7	2	n/a	149	n/a
		(with gap: 152 characters)	(with gap: 34 characters)	(no data)	(no data)	(no data)
Neocryphonectria carpini	CFCC 53027^{T}	–	–	n/a	n/a	n/a
Pseudomastigosporella guizhouensis sp. nov.*	GUCC 406.6^{T}	116	22	n/a	n/a	n/a
Pseudomastigosporella guizhouensis sp. nov.*	GUCC 405.3	116	21	n/a	n/a	n/a
Pseudomastigosporella guizhouensis sp. nov.*	GUCC 405.4	116	21	n/a	n/a	n/a
Pseudomastigosporella guizhouensis sp. nov.*	GUCC 405.8	116	21	n/a	n/a	n/a
		(with gap: 139 characters)	(with gap: 34 characters)	(with gap: 53 characters)	(with gap: 177 characters)	(no data)
Neocryphonectria chinensis	CFCC 53025^{T}	–	–	–	–	n/a
Pseudomastigosporella guizhouensis sp. nov.*	GUCC 406.6^{T}	118	21	75	130	n/a
Pseudomastigosporella guizhouensis sp. nov.*	GUCC 405.3	118	20	76	131	n/a
Pseudomastigosporella guizhouensis sp. nov.*	GUCC 405.4	118	20	n/a	129	n/a
Pseudomastigosporella guizhouensis sp. nov.*	GUCC 405.8	118	20	n/a	132	n/a
		(with gap: 333 characters)	(with gap: 34 characters)	(with gap: 200 characters)	(with gap: 177 characters)	(no data)
Neocryphonectria chinensis	CFCC 53029	–	–	–	–	n/a
Pseudomastigosporella guizhouensis sp. nov.*	GUCC 406.6^{T}	32	21	66	130	n/a
Pseudomastigosporella guizhouensis sp. nov.*	GUCC 405.3	32	20	67	131	n/a
Pseudomastigosporella guizhouensis sp. nov.*	GUCC 405.4	32	20	n/a	129	n/a
Pseudomastigosporella guizhouensis sp. nov.*	GUCC 405.8	32	20	n/a	132	n/a
		ITS	(no data)	(no data)	*tef1*	*tub2*

		(1–636 characters) (with gap: 142 characters)	(no data)	(no data)	(637–1144 characters) (with gap: 195 characters)	(1145–1797 characters) (with gap: 139 characters)
*Diaporthe juglandigena sp. nov.**	GUCC 422.16^{T}	–	n/a	n/a	–	–
*Diaporthe juglandigena sp. nov.**	GUCC 422.161	0	n/a	n/a	0	0
Diaporthe chimonanthi	HGUP191001	18	n/a	n/a	n/a	5
Diaporthe chimonanthi	HGUP192087	23	n/a	n/a	n/a	2
Diaporthe caryae	CFCC 52563^{T}	2	n/a	n/a	6	17
Diaporthe caryae	PSCG520	4	n/a	n/a	6	30
		(with gap: 94 characters)	(no data)	(no data)	(with gap: 307 characters)	(with gap: 150 characters)
Diaporthe eucommiigena sp. nov.*	GUCC 420.9^{T}	–	n/a	n/a	–	–
Diaporthe eucommiigena sp. nov.*	GUCC 420.19	0	n/a	n/a	0	0
Diaporthe passiflorae	CBS 132527^{T}	11	n/a	n/a	23	13
Diaporthe malorum	CAA734^{T}	15	n/a	n/a	19	13
Diaporthe malorum	CAA740	15	n/a	n/a	19	13
Diaporthe malorum	CAA752	15	n/a	n/a	19	13
		(with gap: 124 characters)	(no data)	(no data)	(with gap: 179 characters)	(with gap: 254 characters)
Diaporthe dejiangensis sp. nov.*	GUCC 421.2^{T}	–	n/a	n/a	–	–
Diaporthe dejiangensis sp. nov.*	GUCC 421.21	0	n/a	n/a	0	0
Diaporthe eres	CBS 138594^{T}	4	n/a	n/a	6	6
Diaporthe eres	CAA801	3	n/a	n/a	7	7
Diaporthe cotoneastri	CBS 439.82^{T}	7	n/a	n/a	5	13
		(with gap: 63 characters)	(no data)	(no data)	(with gap: 137 characters)	(with gap: 137 characters)
Diaporthe tongrensis sp. nov.*	GUCC 421.10^{T}	–	n/a	n/a	–	–
Diaporthe tongrensis sp. nov.*	GUCC 421.101	0	n/a	n/a	0	0
Diaporthe phragmitis	CBS 138897^{T}	8	n/a	n/a	n/a	14
		(with gap: 106 characters)	(no data)	(no data)	(with gap: 146 characters)	(with gap: 149 characters)
Diaporthe araliae-chinensis sp. nov.*	GUCC 412.7^{T}	–	n/a	n/a	–	–
Diaporthe araliae-chinensis sp. nov.*	GUCC 412.71	0	n/a	n/a	3	0
Diaporthe araliae-chinensis sp. nov.*	GUCC 412.17	0	n/a	n/a	3	0
Diaporthe lithocarpus	CGMCC 3.15175^{T}	7	n/a	n/a	15	11
Diaporthe lithocarpus	CGMCC 3.151777	9	n/a	n/a	11	n/a
		(with gap: 94 characters)	(no data)	(no data)	(with gap: 177 characters)	(with gap: 215 characters)
Diaporthe hyperici sp. nov.*	GUCC 414.4^{T}	–	n/a	n/a	–	–
Diaporthe hyperici sp. nov.*	GUCC 414.14	0	n/a	n/a	0	2

Diaporthe caulivora	CBS 127268^{T}	17	n/a	n/a	30	11
Diaporthe caulivora	Dip1	17	n/a	n/a	29	n/a
Diaporthe caulivora	Dpc11	17	n/a	n/a	29	n/a
		ITS (1–572 characters) (with gap:34 characters)	**LSU (573–1423 characters) (with gap:11 characters)**	***rpb2* (1424–2460 characters) (with gap:279 characters)**	***tef1* (2461–2861 characters) (no data)**	***tub2* (2862–3354 characters) (no data)**
Gnomoniopsis rosae	CBS 145085	–	–	–	(no data)	(no data)
*Gnomoniopsis rosae**	GUCC 408.7	0	0	0	n/a	n/a
*Gnomoniopsis rosae**	GUCC 408.17	0	0	0	n/a	n/a
		ITS (1–595 characters) (with gap:40 characters)	**LSU (596–1767 characters) (with gap:390 characters)**	**(no data)** n/a	***tef1* (1768–2165 characters (with gap:135 characters)**	**(no data)** n/a
Coniella quercicola	CBS 904.69^{T}	–	–	n/a	–	n/a
Coniella quercicola	CBS 283.76	0	0	n/a	1	n/a
Coniella quercicola	CPC 12133	1	n/a	n/a	5	n/a
*Coniella quercicola**	GUCC 414.2	0	0	n/a	10	n/a
*Coniella quercicola**	GUCC 414.21	0	0	n/a	10	n/a
*Coniella quercicola**	GUCC 412.3	0	0	n/a	18	n/a
*Coniella quercicola**	GUCC 405.6	0	0	n/a	7	n/a
*Coniella quercicola**	GUCC 405.16	0	0	n/a	6	n/a

Figures

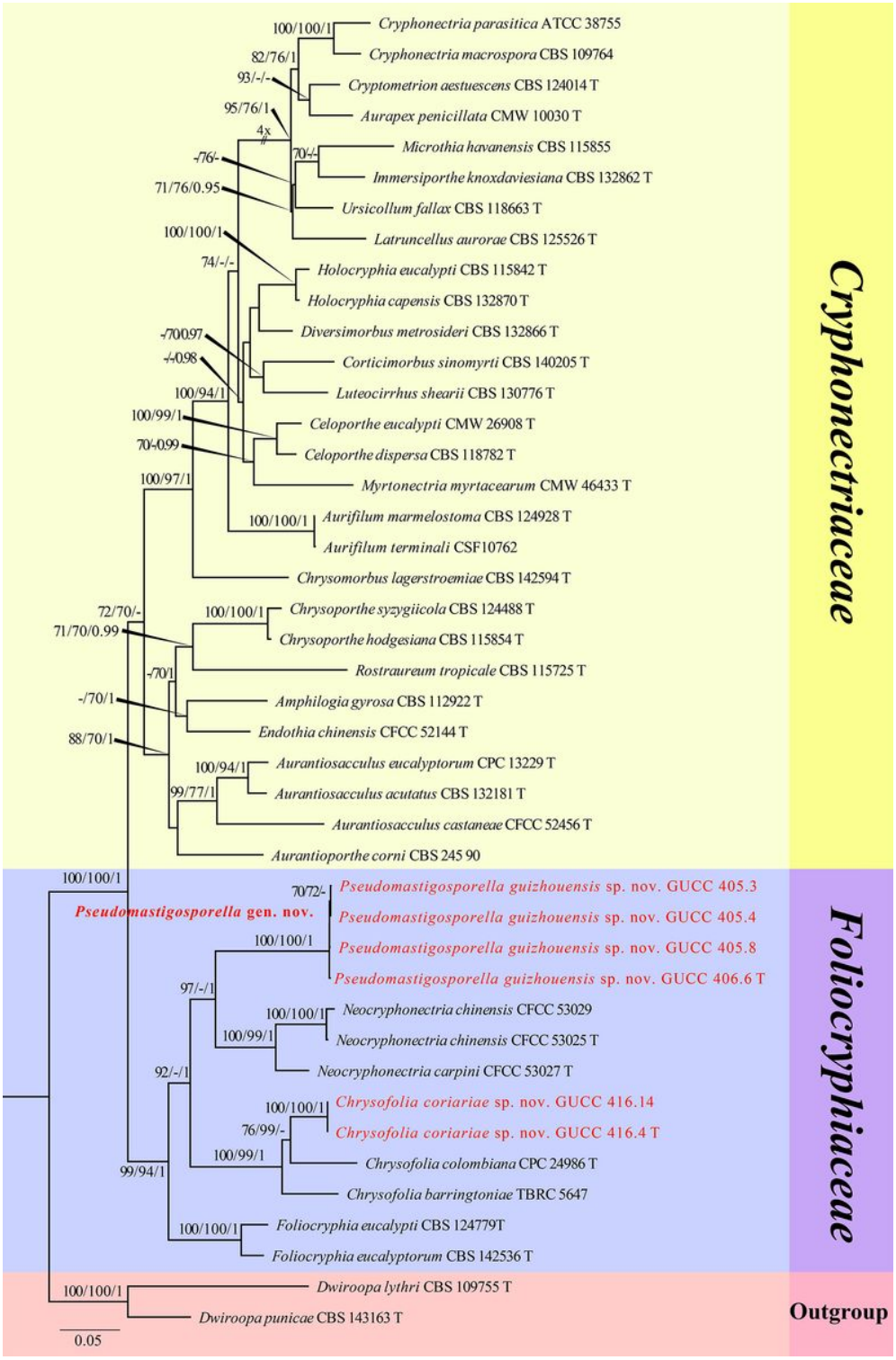

Figure 1

Phylogram generated from RAxML analysis of a concatenated ITS-LSU-*rpb2-tef1-tub2* sequence dataset to represent the phylogenetic relationships of taxa in *Foliocryphiaceae* and *Cryphonectriaceae*. The tree was rooted with *Dwiroopa lythri* (CBS 109755, ex-type strain) and *Dw. punicae* (CBS 143163, ex-type strain). Bootstrap support values for ML and MP equal to or greater than 70% and Bayesian posterior probabilities equal to or higher than 0.95 PP are indicated above the nodes as ML/MP/PP. Support values lower than 70% ML/MP and 0.95 PP are indicated by a hyphen (-).The newly generated sequences are indicated in red.

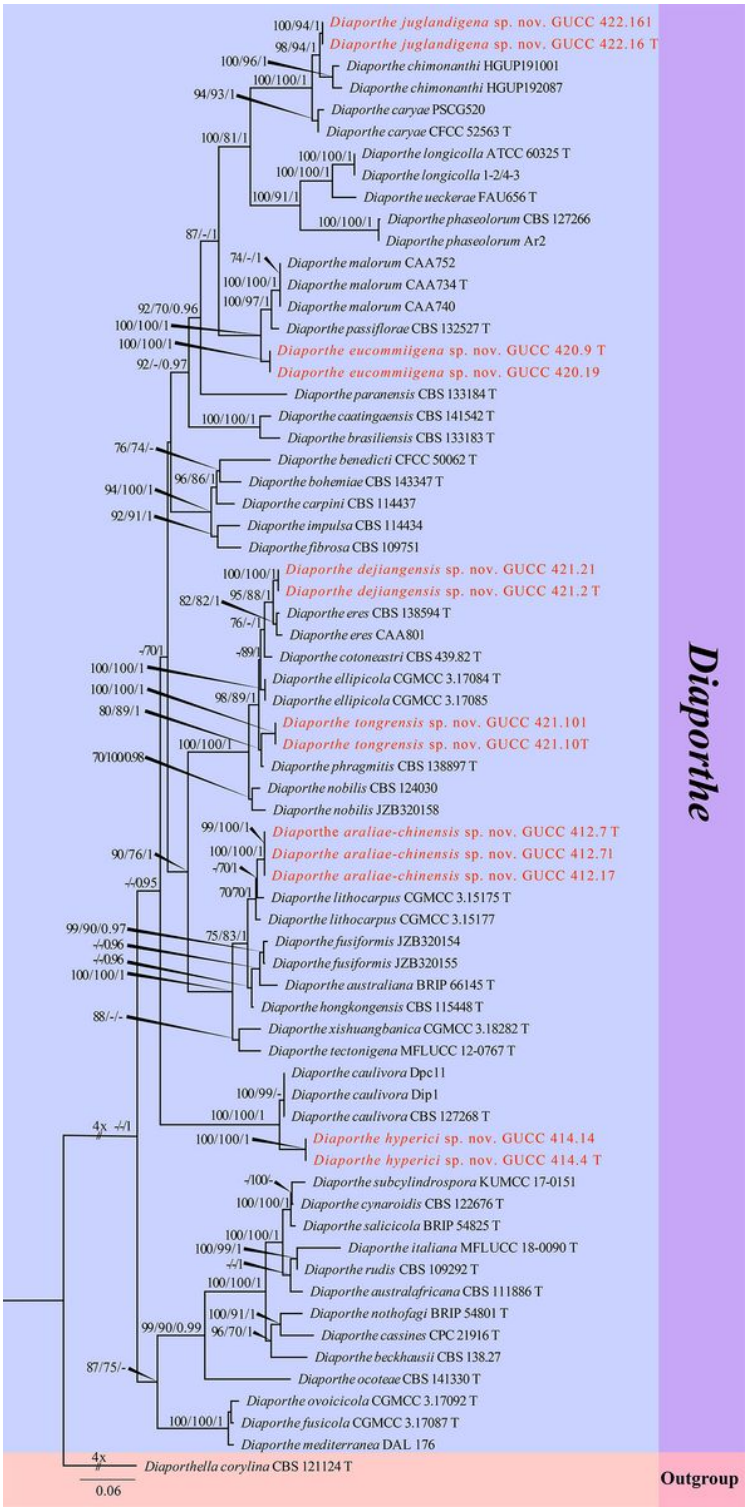

Figure 2

Phylogram generated from RAxML analysis of a concatenated ITS-*tef1*-*tub2*sequence dataset to represent the phylogenetic relationships of taxa in *Diaporthe*. The tree was rooted with *Diaporthella corylina* (CBS 121124, ex-type strain). Bootstrap support values for ML and MP equal to or greater than 70% and Bayesian posterior probabilities equal to or higher than 0.95 PP are indicated above the nodes as ML/MP/PP. Support values lower than 70% ML/MP and 0.95 PP are indicated by a hyphen (-). The newly generated sequences are indicated in red.

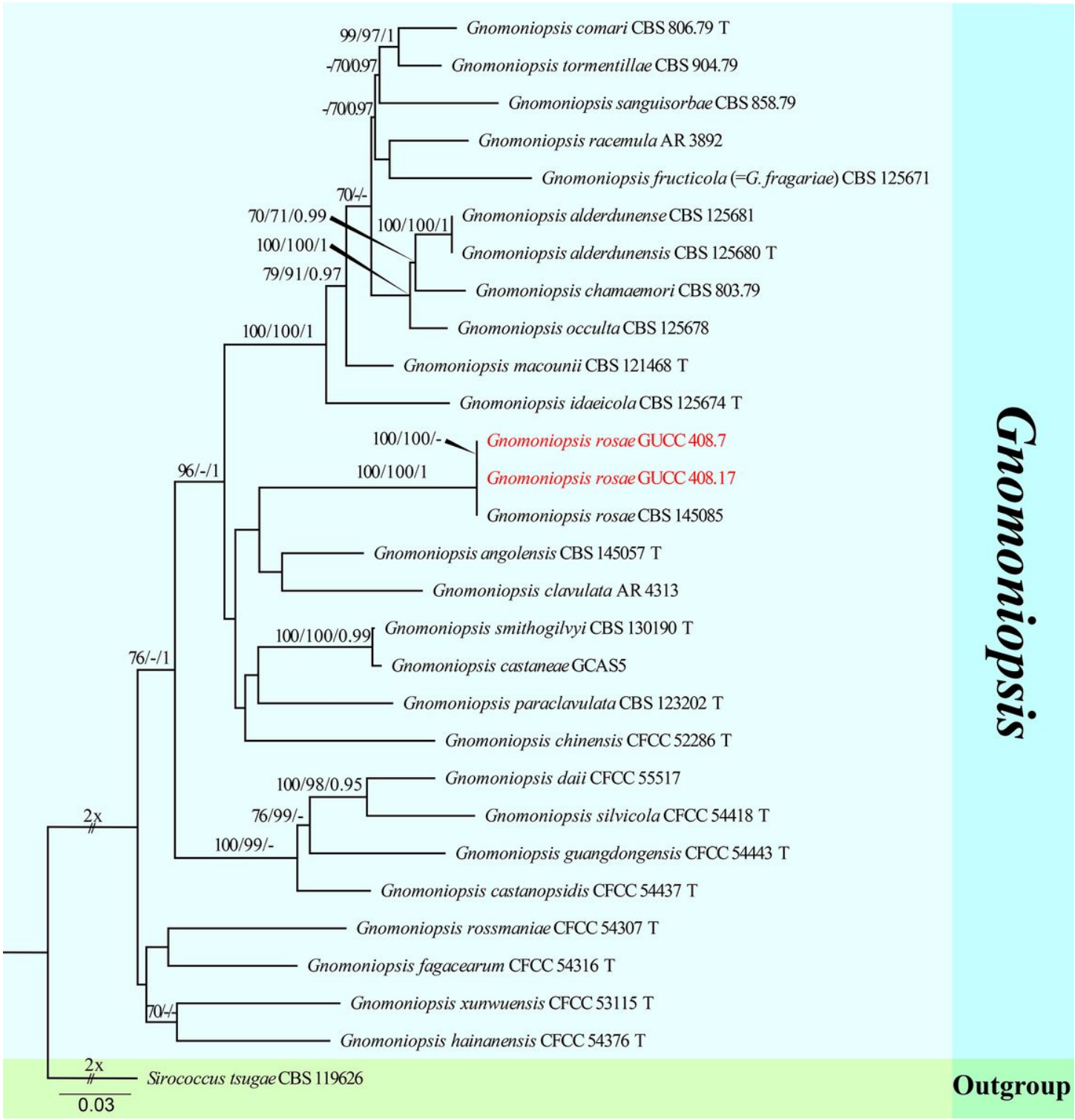

Figure 3

Phylogram generated from RAxML analysis of a concatenated ITS-LSU-*rpb2-tef1-tub2*sequence dataset to represent the phylogenetic relationships of taxa in *Gnomoniopsis*. The tree was rooted with *Sirococcus tsugae* (CBS 119626). Bootstrap support values for ML and MP equal to or greater than 70% and the Bayesian posterior probabilities equal to or higher than 0.95 PP are indicated above the nodes as ML/MP/PP. Support values lower than 70% ML/MP and 0.95 PP are indicated by a hyphen (-). The newly generated sequences are indicated in red.

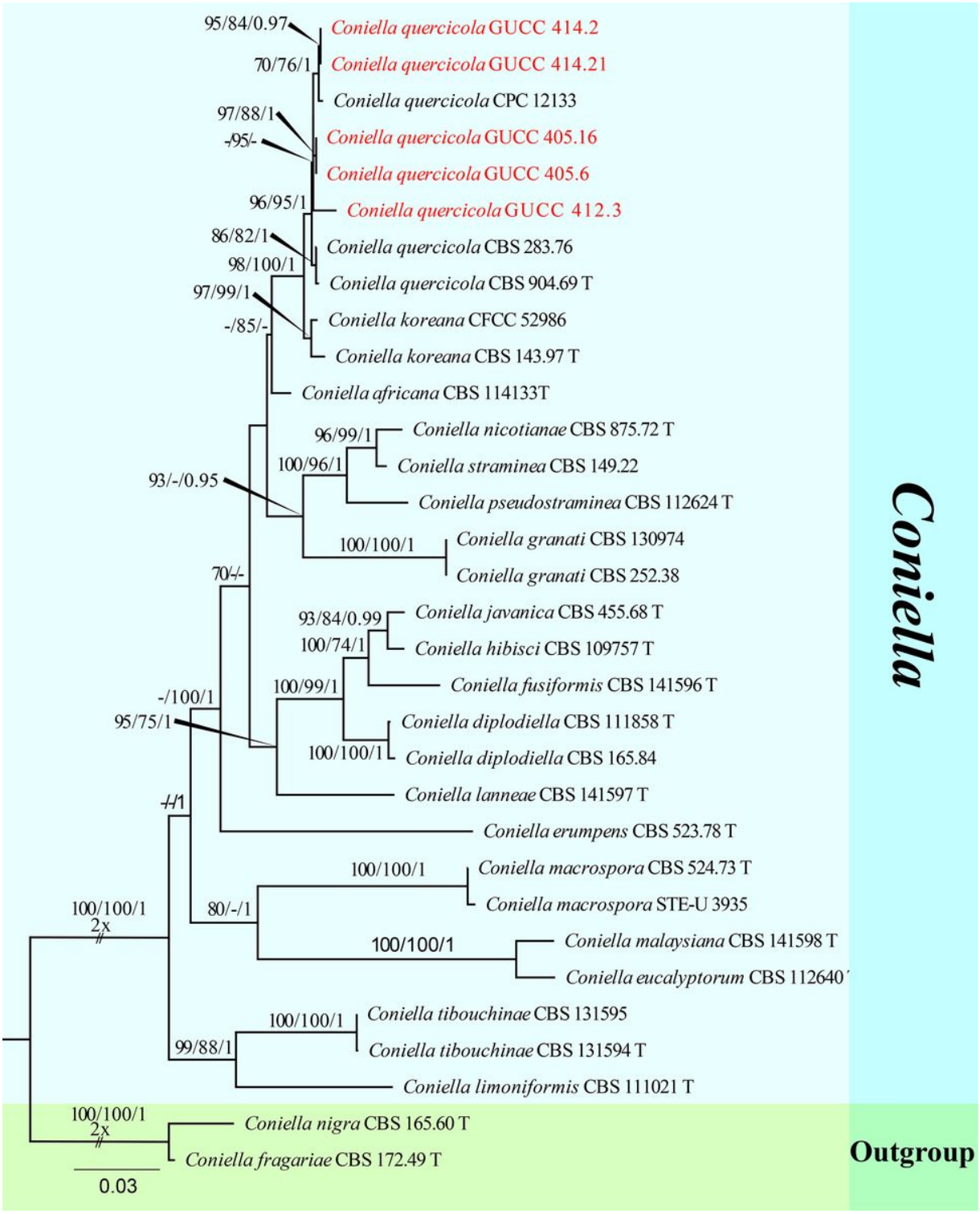

Figure 4

Phylogram generated from RAxML analysis of a concatenated ITS-LSU-*tef1* sequence dataset to represent the phylogenetic relationships of taxa in *Coniella*. The tree was rooted with *C. fragariae* (CBS 172.49, ex-type strain) and *C. nigra* (CBS 165.60, ex-type strain). Bootstrap support values for ML and MP equal to or greater than 70% and the Bayesian posterior probabilities equal to or higher than 0.95 PP are indicated above the nodes as ML/MP/PP. Support values lower than 70% ML/MP and 0.95 PP are indicated by a hyphen (-). The newly generated sequences are indicated in red.

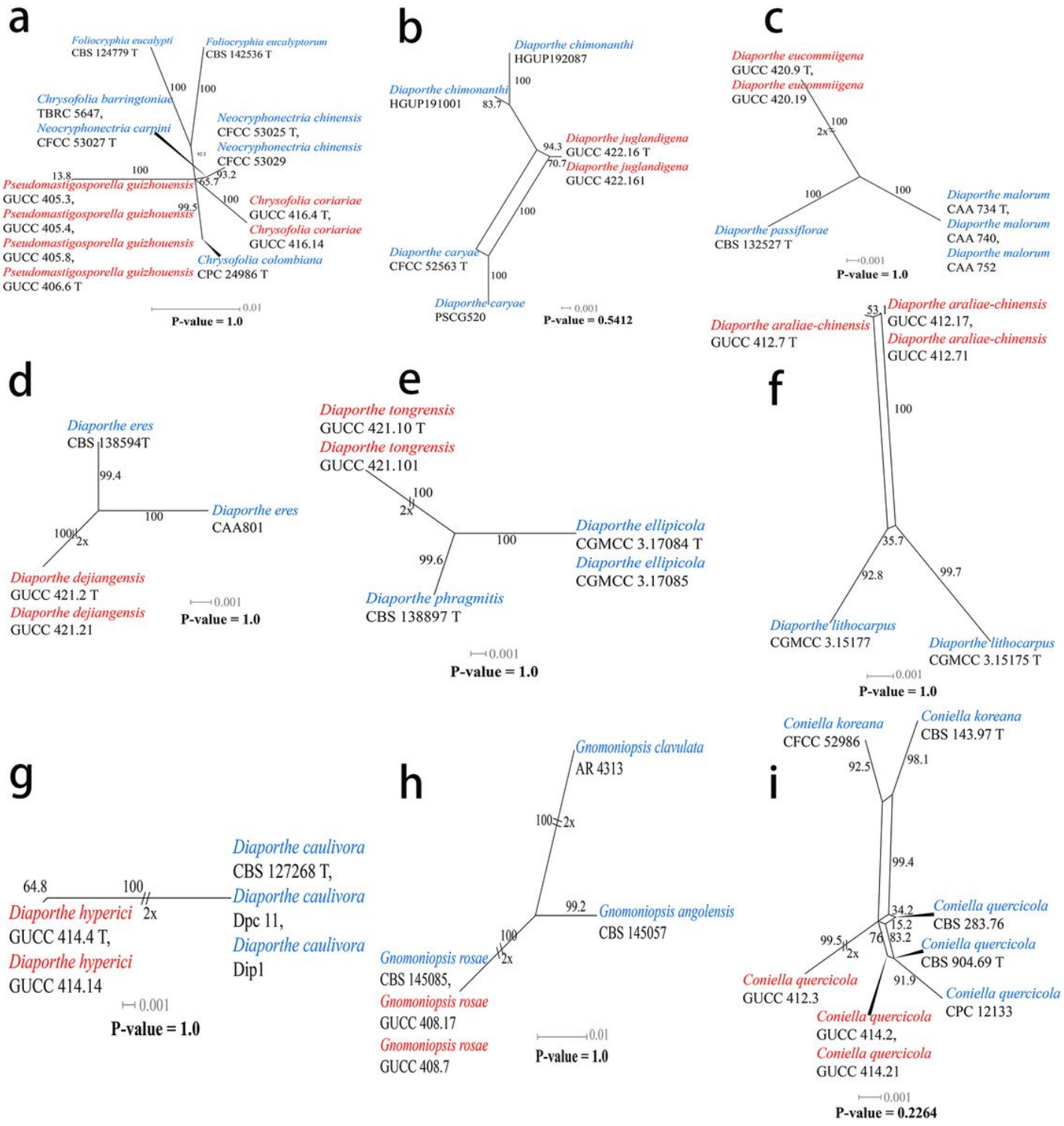

Figure 5

Results of the pairwise homoplasy index (PHI) test of closely related species using both LogDet transformation and splits decomposition. Our strains are indicated in red, other involved strains are indicated in blue.

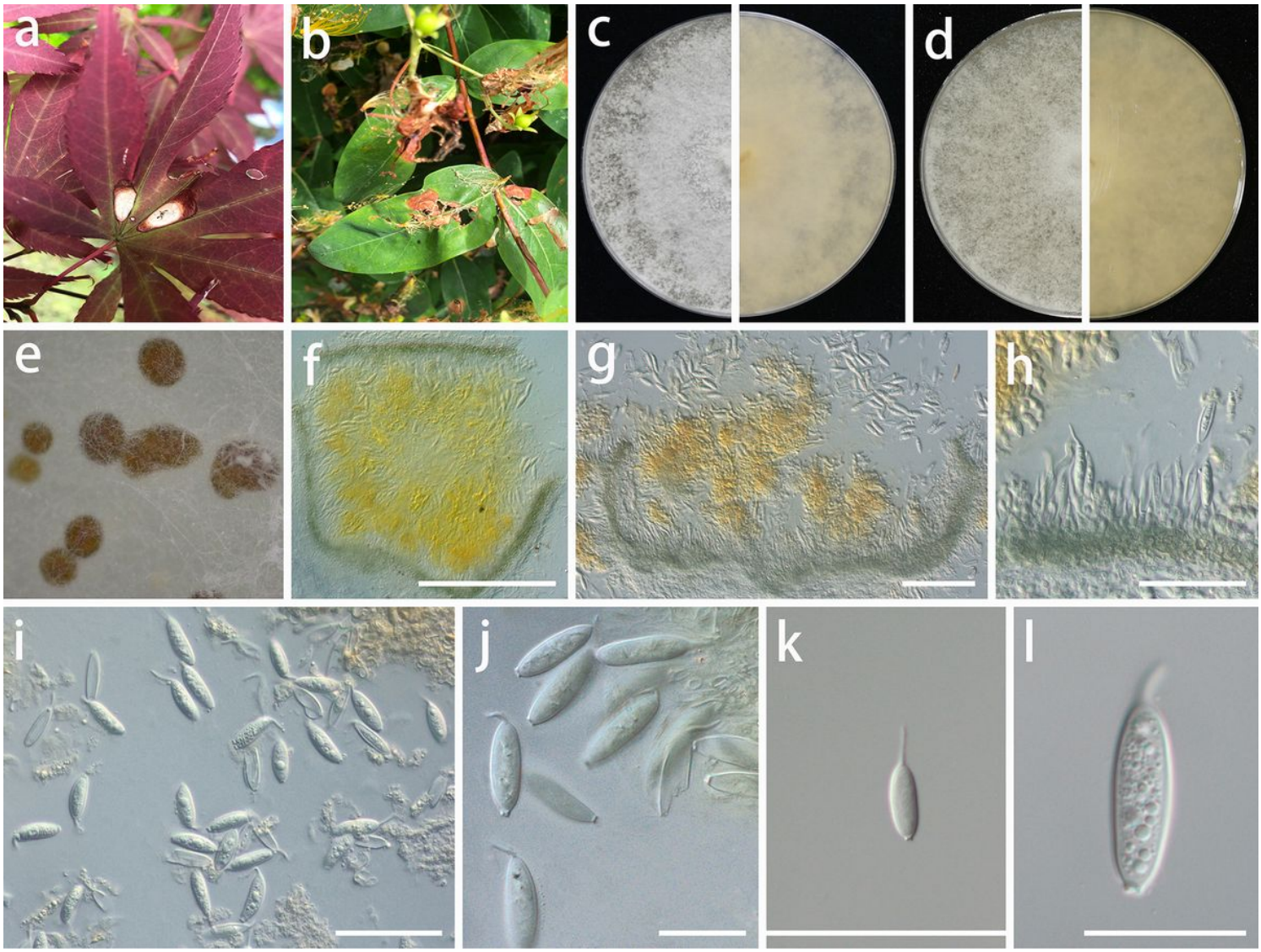

Figure 6

Pseudomastigosporellaguizhouensis (GUCC 406.6). Hosts: **a** *Hypericum patulum*; **b** *Acer palmatum*. **c** Colony on PDA after 2 wk at 25 °C(left: above, right: reverse). **d** Colony on OA after 2 wk at 25 °C (left: above, right: reverse). **e** Mass of conidia. **f** Conidioma. **g–h** Conidiomata and conidiogenous cells. **i–l** Conidia. Scale bars: **f–i** = 50 μm; **j–l**= 10 μm.

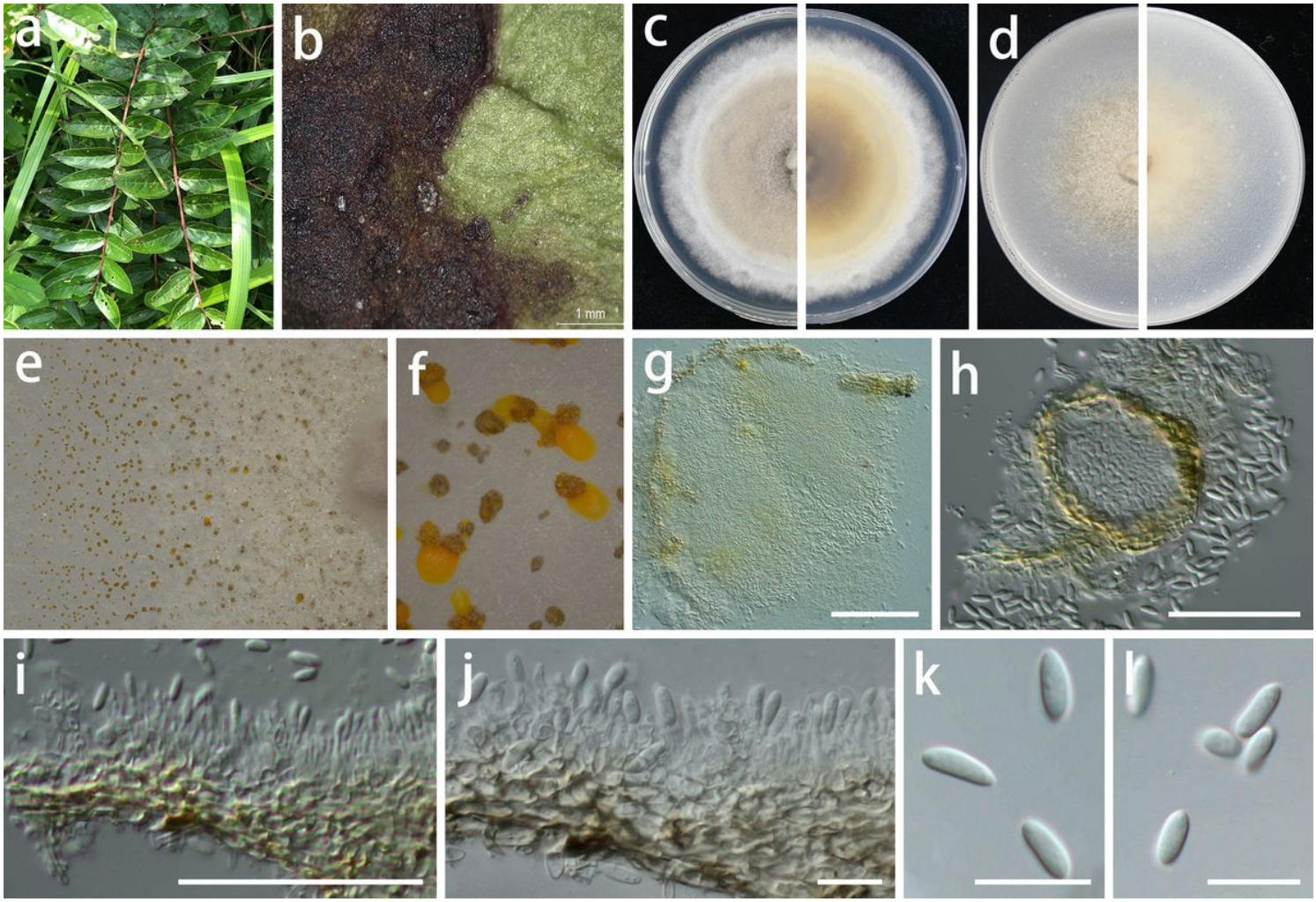

Figure 7

Chrysofolia coriariae (GUCC 416.4). **a–b**Host: *Coriaria nepalensis*. **c**Colony on PDA after 2 wk at 25 °C (left: above, right: reverse). **d** Colony on OA after 2 wk at 25 °C (left: above, right: reverse). **e–f** Conidial masses. **g–h** Conidiomata. **i–j** Conidiogenous cells. **k–l** Conidia. Scale bars: **g–i** = 50 µm; **j–l** = 10 µm.

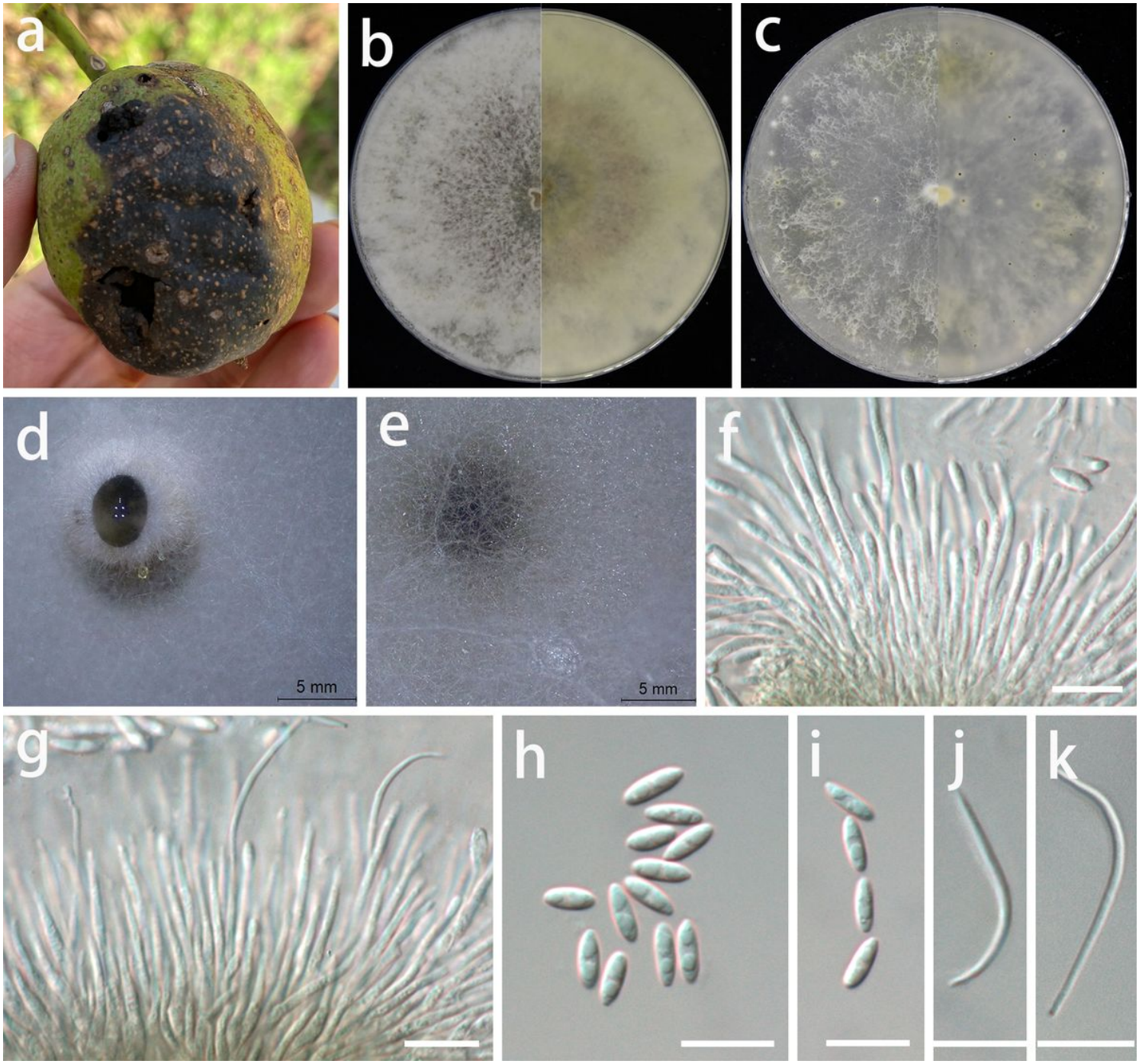

Figure 8

Diaporthe juglandigena (GUCC 422.16). **a** Host: *Juglans regia*. **b** Colony on PDA after 2 wk (left: above, right: reverse). **c** Colony on OA after 2 wk (left: above, right: reverse). **d–e** Mass of conidia. **f–g**Conidiogenous cells. **h–i** Alpha conidia. **j–k** Beta conidia. Scale bars: **f–k** = 10 μm.

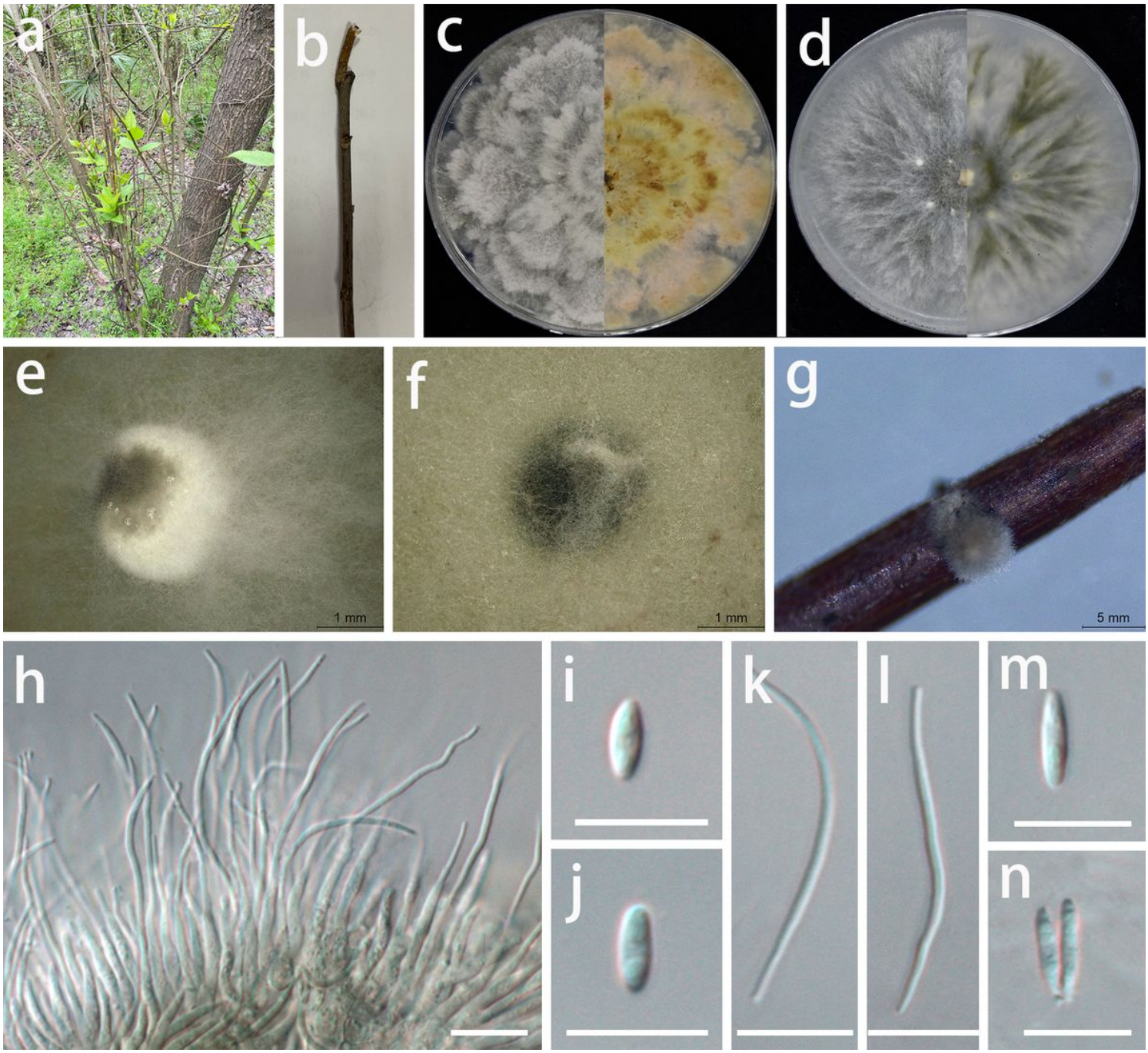

Figure 9

Diaporthe eucommiigena (GUCC 420.9). **a–b** Host: *Eucommia ulmoides*. **c** Colony on PDA after 2 wk at 25 °C (left: above, right: reverse). **d** Colony on OA after 2 wk at 25 °C (left: above, right: reverse). **e–g** Mass of conidia. **h** Conidiogenous cells. **i–j**Alpha conidia. **k–l** Beta conidia. **m–n** Gamma conidia. Scale bars: **h–n** = 10 μm.

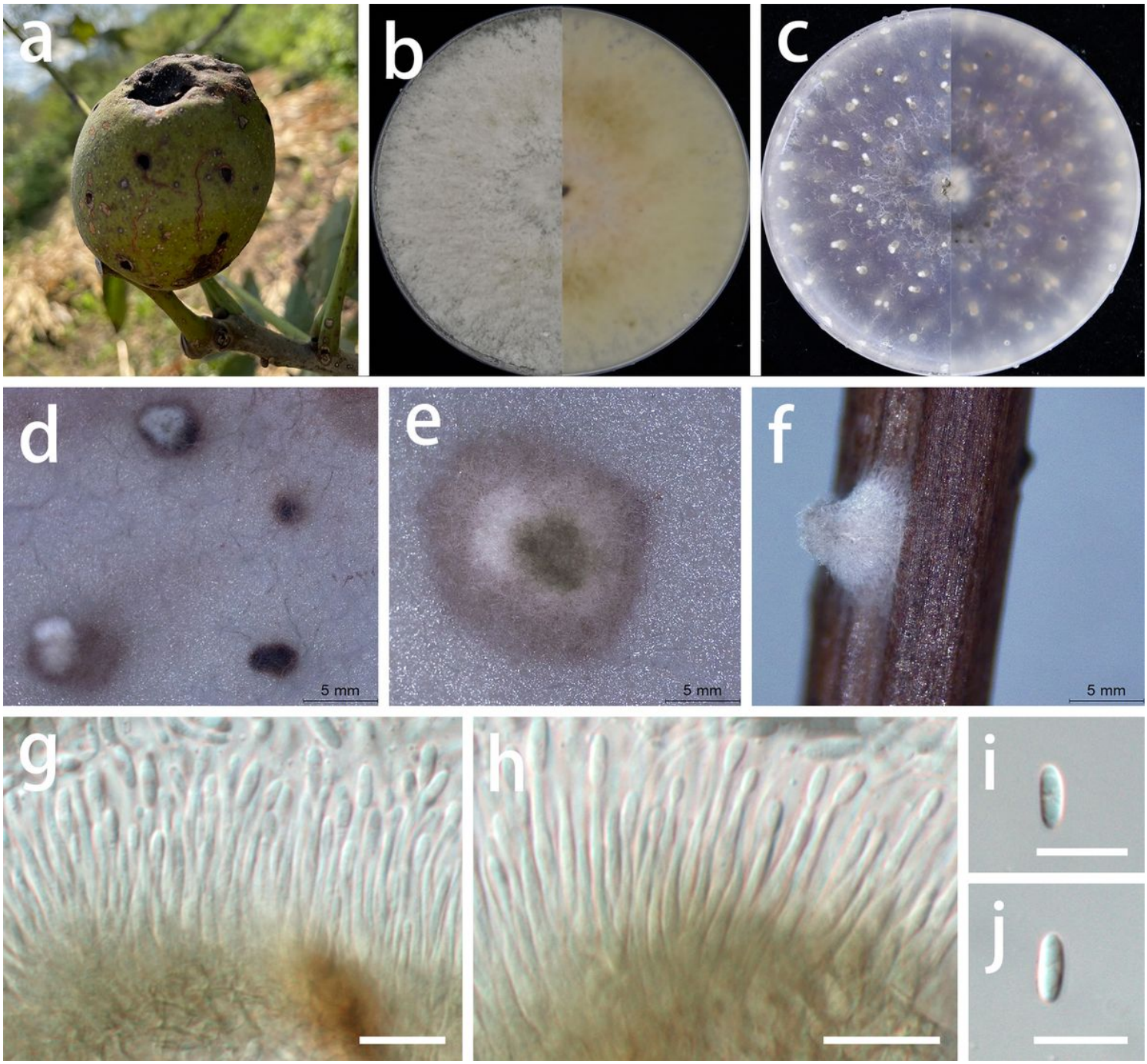

Figure 10

Diaporthe dejiangensis (GUCC 421.2). **a** Host: *Juglans regia*. **b** Colony on PDA after 2 wk at 25 °C (left: above, right: reverse). **c**Colony on OA after 2 wk at 25 °C (left: above, right: reverse). **d–f** Mass of conidia. **g–h** Conidiogenous cells. **i–j** Alpha conidia. Scale bars: **g–j** = 10 μm.

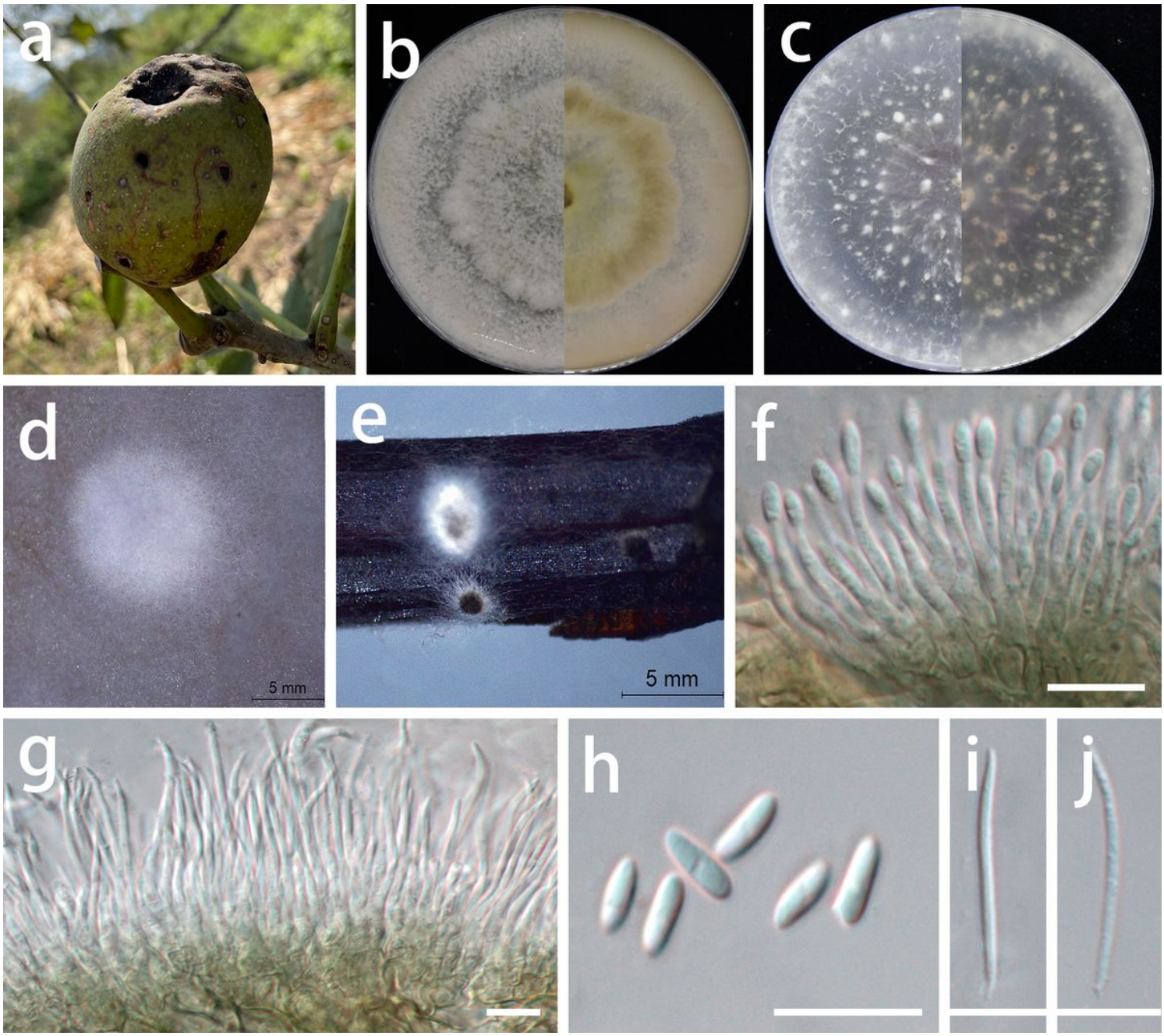

Figure 11

Diaporthe tongrensis (GUCC 421.10). **a** Host: *Juglans regia*. **b** Colony on PDA after 2 wk at 25 °C (left: above, right: reverse). **c** Colony on OA after 2 wk at 25 °C (left: above, right: reverse). **d–e** Mass of conidia. **f–g**Conidiogenous cells. h Alpha conidia. **i–j** Beta conidia. Scale bars: **f–j**= 10 μm.

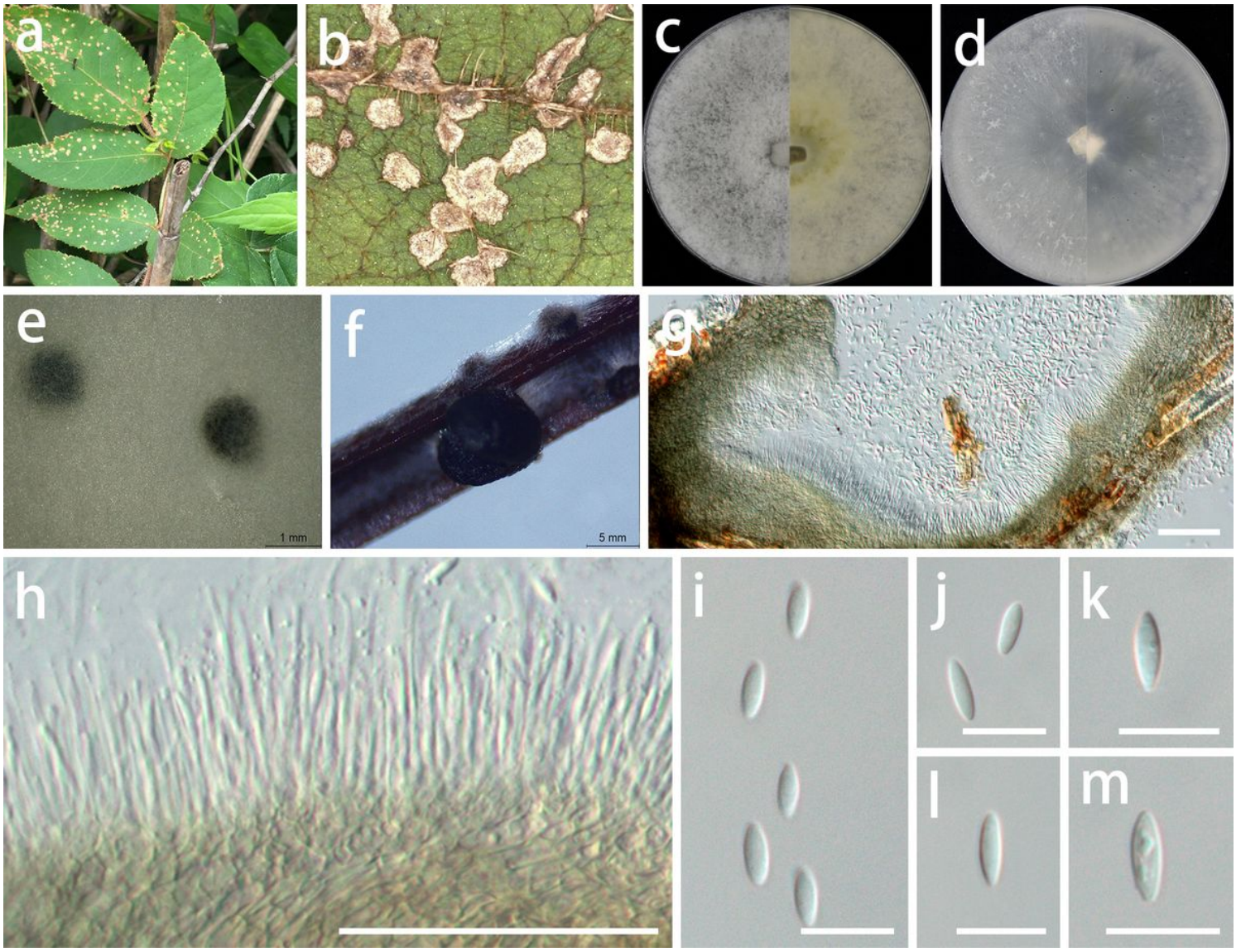

Figure 12

Diaporthe araliae-chinensis (GUCC 412.7). **a–b** Host: *Aralia chinensis*. **c**Colony on PDA after 2 wk at 25 °C (left: above, right: reverse). **d** Colony on OA after 2 wk at 25 °C (left: above, right: reverse). **e–f** Mass of conidia on OA and pine needle. **g** Conidioma. **h** Conidiogenous cells. **i–m** Alpha conidia. Scale bars: **g–h**= 50 µm; **i–m** = 10 µm.

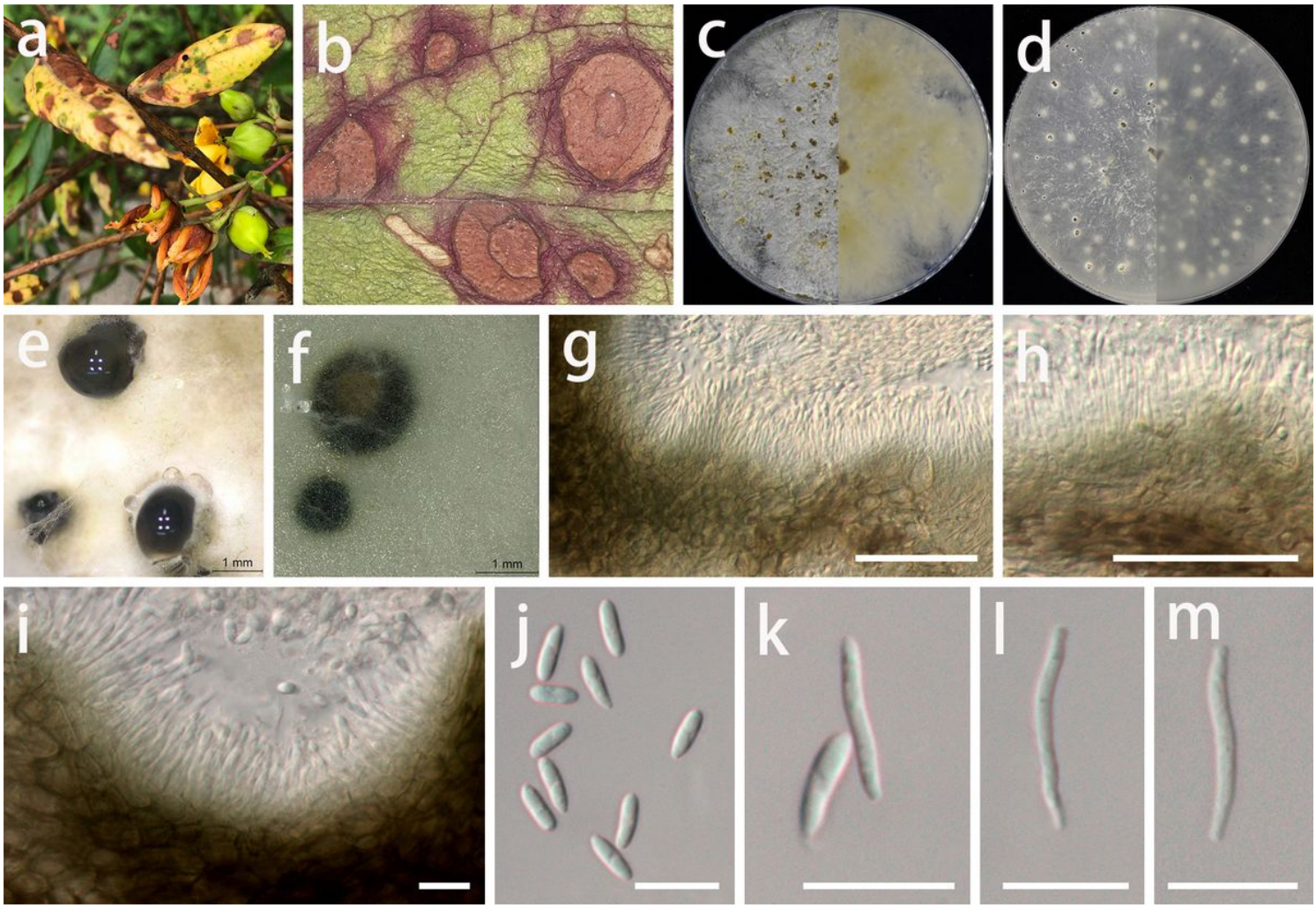

Figure 13

Diaporthe hyperici (GUCC 414.4). **a–b** Host: *Hypericum patulum*. **c** Colony on PDA after 2 wk at 25 °C (left: above, right: reverse). **d**Colony on OA after 2 wk at 25 °C (left: above, right: reverse). **e–f** Mass of conidia. **g–i** Conidiogenous cells. **j** Alpha conidia. **k**Alpha and beta conidia. **l–m** Beta conidia. Scale bars: **g–h** = 50 µm; **i–m** = 10 µm.

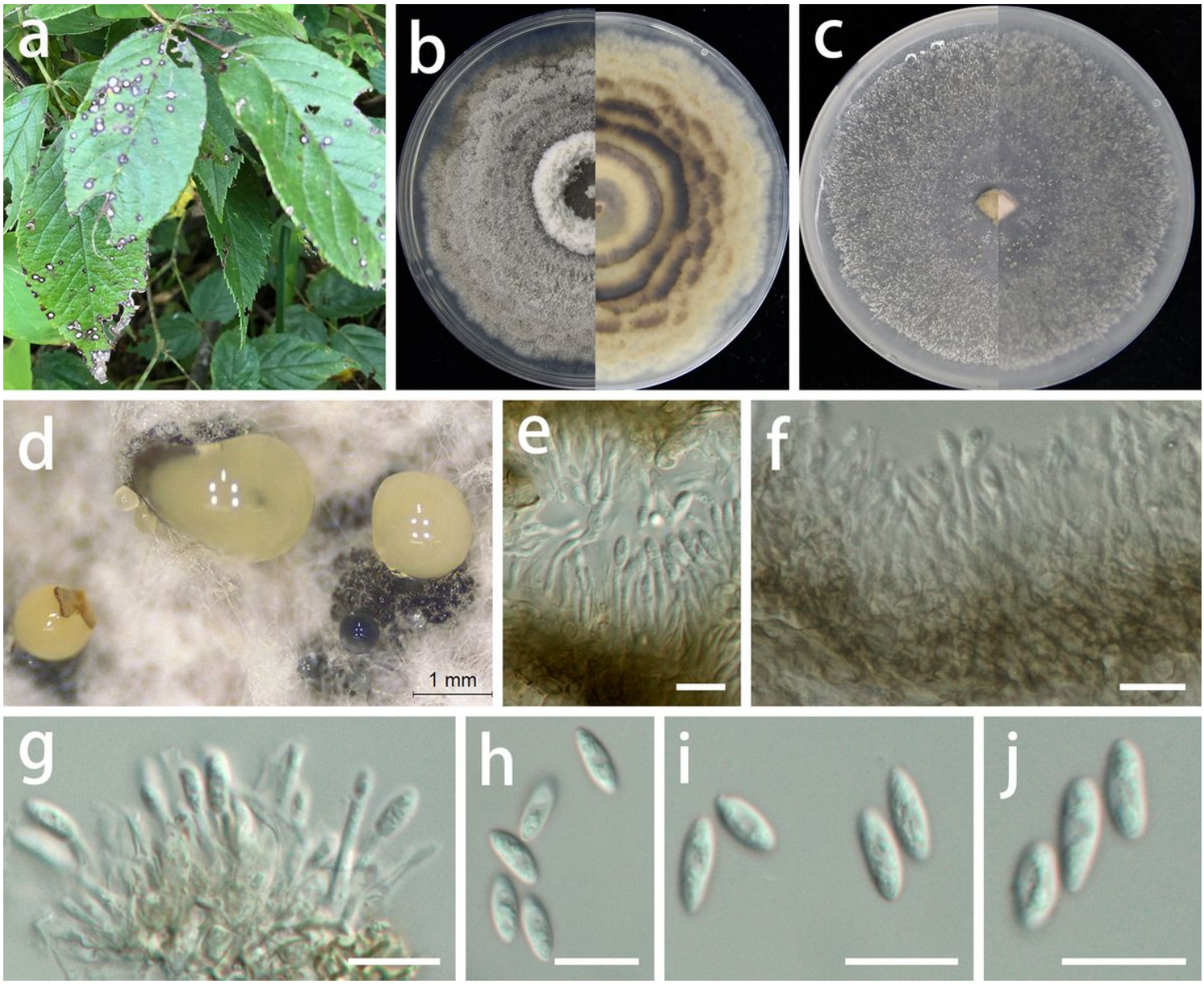

Figure 14

Gnomoniopsis rosae (GUCC 408.7). **a** Host: *Rose sp.*. **b** Colonies on PDA after 2 wk at 25 °C (left: above, right: reverse). **c** Colony on OA after 2 wk at 25 °C (left: above, right: reverse). **d** Mass of conidia. **e** Conidiomata. **f–g**Conidiogenous cells. **h–j** Conidia. Scale bars: **e–j** = 10 µm.

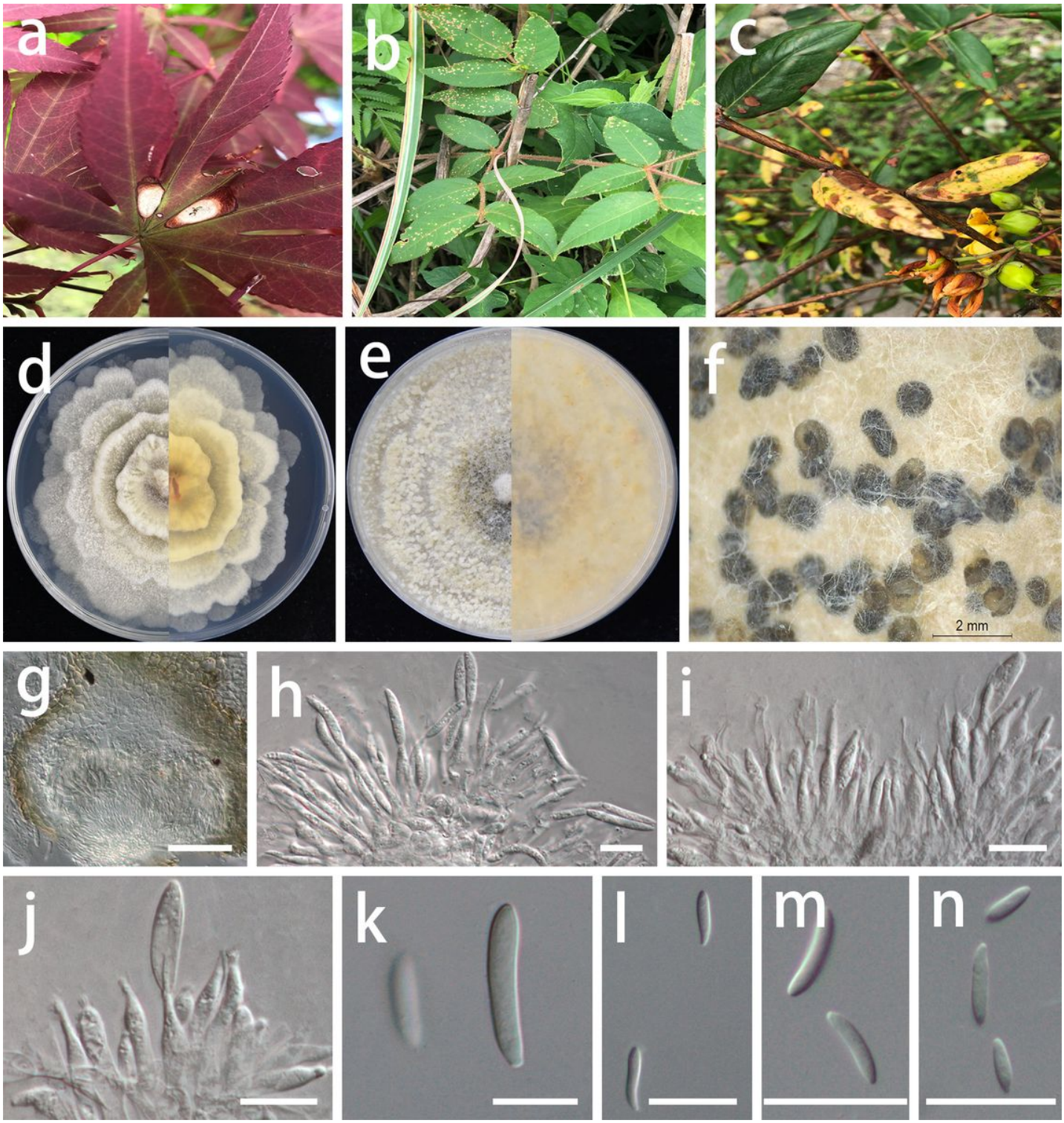

Figure 15

Coniella quercicola (GUCC 412.3). Hosts. a: *Acer palmatum*; b: *Aralia chinensis*; c: *Hypericum patulum*. d: Colony on PDA after 2 wk 25 °C(left: above, right: reverse). e: Colony on OA after 2 wk 25 °C(left: above, right: reverse). f: Mass of conidia. g: Conidioma. h–j: Conidiogenous cells. k–n: Conidia. Scale bars: g = 50 μm; h–n = 10 μm.

Supplementary Files

This is a list of supplementary files associated with this preprint. Click to download.

- Fig.1Foliocryphiaceae.nex
- Fig.2Diaporthe.nex
- Fig.3Gnomoniopsis.nexus
- Fig.4Coniella.nexus